ELICE16INDURES ®: a plant immune-priming activator targeting jasmonate metabolism via TIFY and RHOMBOID proteins in *Hordeum vulgare*

Géza Hegedűs[1,2], Márta Kiniczky[1], Ágnes Nagy[1], Péter Pekker[3], Balázs Lang [4], Szilvia Kleineizel[4], József Péter Pallos[1], Zsófia Thomas-Nyári[1], Kincső Decsi[5], Barbara Kutasy[5], Kinga Székvári[2], Ákos Juhász[6], Eszter Virág[1,2,7]*

[1]Research Institute for Medicinal Plants and Herbs Ltd. Luppaszigeti str 4, Budakalász, Hungary, 2011
[2]EduCoMat Ltd., Iskola str 12A, Keszthely, Hungary, 8360
[3]University of Pannonia, Research Institute of Biomolecular and Chemical Engineering, Nanolab, Egyetem str 10, Veszprém, Hungary, 8200
[4]Plant-Art Research Ltd, Ébner György Köz 5, Budaörs, Hungary, 2040
[5] Department of Plant Physiology and Plant Ecology, Campus Keszthely, Hungarian University of Agriculture and Life Sciences Georgikon, 7 Festetics Str., Keszthely, Hungary, 8360
[6] Department of Microbiology and Applied Biotechnology, Institute of Genetics and Biotechnology, Hungarian University of Agriculture and Life Sciences, Páter Károly street 1, Gödöllő, Hungary, 2100
[7]Department of Molecular Biotechnology and Microbiology, Institute of Biotechnology, Faculty of Science and Technology, University of Debrecen, Egyetem Square 1, Hungary, 4032

*Corresponding author: virag.e@gynki.hu, eszterandreavirag@gmail.com

Short title: Priming response to ELICE16INDURES® plant conditioner

One-sentence summary: ELICE16INDURES® is a plant conditioner agent with a high amount of allelochemicals encapsulated into small multilamellar liposomes and found as an immune priming activator tested in *H. vulgare* field and phytotron cultures.

The author responsible for distribution of materials integral to the findings presented in this article in accordance with the policy described in the Instructions for Authors (https://academic.oup.com/plcell/pages/General-Instructions) is: Eszter Virág (virag.e@gynki.hu).

Abstract

Priming activity of plant-based allelochemicals is advanced research nowadays meaning a high potential in sustainable agriculture. The ELICE16INDURES® (RIMPH LTD, Hungary) plant conditioner of CO_2 botanical extracts is rich in plant-active ingredients such as phenolic compounds, alkaloids, and flavonoids formulated in small multilamellar liposomes. This product was investigated *in autumn barley (Hordeum vulgare)*. Field experiments of ELICE16INDURES showed augmented NDVI values interconnected with higher photosynthetic activity and yield increase. Background of the better vitality of plants was investigated by whole genomic gene expression profiling and showed an enhanced response to wounding, jasmonic acid, oxidative detoxification, and chloroplast activity. Among top50 differentially expressed genes the TIFY domain protein TIFY11B and RHOMBOID-like protein 2 related to JA signaling were up-regulated in field-collected samples. Phytotron experiments of barley were set up to validate and evaluate the transcriptomic effect of ELICE16INDURES. Well-studied priming active agents such as salicylic acid and beta-aminobutyric acid were compared with ELICE16INDURES and confirmed as priming inducer material with positive regulation of TIFY11B, TIFY3B, TIFY9, TIF10A, and RHOMBOID like protein 2 by using NGS GEx and RT-qPCR methods.

1 **INTRODUCTION**

2   The application of natural-based activators is the most innovative and ecologically

3 safe resolution to increase crop vitality and production. Nowadays sustainable agricultural

4 production and preservation of biodiversity in agricultural fields pay great attention

5 worldwide therefore the development of alternative plant protection is in focus avoiding the

6 use of chemicals: pesticides, nutrients, or soil improvers (Du Jardin, 2015). Many companies

7 are developing products of biologically active agents (Calvo et al., 2014; Sharma et al., 2014)

8 based on plant signaling molecules so-called „metabolic enhancers" or "biostimulants"

9 among which natural vitamins, phytohormones, amino acids, and their derivatives are the

10 most significant (Ugena et al., 2018). To improve yield and abiotic stress tolerance in

11 agriculturally important cereal cultures the use of biostimulants is a promising approach,

12 however, less applied in practice than synthetic ones.

13   The responses to biostimulants were first studied in *Arabidopsis thaliana* (*A. thaliana*,

14 mouse-ear cress) because this plant has one of the smallest plant genomes (Toscano et al.,

15 2018; Geelen and Xu, 2020). In this experiment, 127 genes showed at least 3-fold activity

16 against an untreated plant under the influence of a commercially available biostimulant

17 formulation. Selivanova et al. (2015) investigated the physiological processes of cucumber

18 plants under the influence of several commercially available biostimulant products. The

19 results of the experiment showed an increased plant metabolism as a result of the

20 treatment, which in turn increased yields. Klokić et al. (2020) examined the effect of

21 biostimulants on tomato yield characteristics. As a result of the experiment, it can be

22 concluded that the treatments with 10 different biostimulants influenced the characteristics

23 of the fruits, such as the total phenol and flavonoid content and the total antioxidant

24 capacity (Klokić et al., 2020). Špoljarevic et al. examined the activity of antioxidants in

25 strawberry (*Fragaria x ananassa Duch*) leaves in two biostimulant treatments with two

26 nutrient replenishment. The specific activities of guaiacol peroxidase (GPX), catalase (CAT),

27 ascorbate peroxidase (APX) and glutathione reductase (GR) were investigated in leaves.

28 Based on the results, it may be concluded that the values of antioxidant enzymes were

29 higher in the leaves after treatment with biostimulants and reduced nutrient replenishment.

30 APX and GR showed the highest activity in the treated plants, and the strongest relationship

31 was also between these two enzymes, which are enzymes of the ascorbate-glutathione cycle

32 (Špoljarević et al., 2010). Later they summarized the researches on different biostimulants in

33 horticultural plant species with the conclusion of the effects of physiologically active

34 compounds on plants may depend on dose, time of treatment, growth conditions, and plant

35 species. Therefore they suggest intensive research in this field (Parađiković et al., 2019).

36   Some biostimulants may protect plants from a broad range of pathogens by

37 activating the plant immune system (Burketova et al., 2015; Vargas-Hernandez et al., 2017).

38 The effect of these materials lies in not targeting pathogens like pesticides or not directly

39 induce immune response overcoming by pathogenic microbes however, potentiate plant

40 defense mechanism long term, therefore they are called priming-active or imprimatin-

41 compounds (Noutoshi et al., 2012). From the point of view of field usage of biostimulants,

42 priming-active materials are the more cost-effective since the induced resistance may be

43 triggered and optimized. Some natural and synthetic compounds have demonstrated good

44 priming-inducing activity in laboratory and field conditions, such as the nonprotein β-

45 aminobutyric acid (BABA) or the phytohormone salicylic acid (SA) (Beckers and Conrath,

46 2007; Walters et al., 2014). The effect of priming-active elicitors on protection and signaling

47 pathways has already been demonstrated, so its potential use in the field is well-founded

48 and highlighted. From the 20 years of the discovery of these compounds, the mechanisms of

49 plant immune responses are also gaining more and more light and paving the way for new

50 plant protection strategies (Schwessinger and Ronald, 2012).

51   Several plant extracts were used as priming agents among which the seed priming

52 gain in more attention in field crops (Farooq et al., 2019). In these experiments the

53 allelochemicals such as phenolic compounds, alkaloids, terpenoids, flavonoids, saponins, and

54 steroids may act beneficially to plant growth, germination reaching higher vitality and

55 resilience (Narwal, 2006; Adeniyi et al., 2010; Narwal, 2012; Moses et al., 2014; Mujeeb et

56 al., 2014; Latif et al., 2020). For example, the reduction in mortality and high seedling vigor in

57 tomatoes was reported by primed tomato seeds with Azadirachta, Chlorophytum, and Vinca

58 (Prabha et al., 2016). Saponins can enhance nutrient absorption as they are readily soluble in

59 water. Alkaloids, saponins, and phenolic compounds present in the leaves of various plants

60 are involved in the production of antioxidant activities and protect the plants against

61 pathogens (Satish et al., 2007). The strong presence of the above-mentioned phytochemicals

62 was proven in different extracts of garlic cloves (Divya et al., 2017) and their antimicrobial

3

63 properties were also investigated against pathogens such as *Fusarium* and *Aspergillus*

64 species (Olusanmi and Amadi, 2010).

65 An advanced method in priming is the use of nanoparticles in the range of 100-500 nm in

66 size. Although this technology is in little attention, there are some reports on the positive

67 impact of their uptake and nutrient delivery applied in foliar and seed priming as well (Dutta,

68 2018; Abdel-Aziz et al., 2019). However, the priming with nano-size liposomes as

69 macromolecule carriers was not yet been reported in plants. Some studies investigated the

70 use of liposomes to supplement plant growth and overcome acute nutrient deficiency (Karny

71 et al., 2018). The advantage of liposome encapsulation is to reduce the quantity of bioactive

72 compounds to reach the same impact. The product ELICE16INDURES® plant conditioner

73 (Research Institute for Medicinal Plants and Herbs Ltd. Budakalász, Hungary) contains Garlic

74 cloves CO_2 extracts, and a high amount of above-mentioned allelochemicals encapsulated in

75 250-350 nm size multilamellar liposomes.

76   In this study, the transcriptomic effect of ELICE16INDURES was investigated and

77 compared with BABA and SA priming agents in the field and phytotron experiments on

78 autumn barley *(Hordum vulgare).* Chloroplast activity predictions were performed by remote

79 sensing in field cultures. Monitoring the extension of photosynthetic surface in barley

80 cultures by using agro-drone a higher vitality was detected in the ELICE16INDURES treated

81 plots that were manifested also in augmented crop yield.

82

83 **RESULTS AND DISCUSSION**

84

85 **Testing of ELICE16INDURES in field experiments**

86 **Determination of NDVI in field populations of *H. vulgare***

87   The NDVI value provides information on the photosynthetic activity of plants (Kalbi et

88 al., 2014), i.e. it examines how much of the light in the photosynthetic wavelength range can

89 be used by the plant. NDVI gives a picture of the differences in vegetation activity and

90 vegetation rate within the field. This provides useful information for assessing heterogeneity

91 within the field and may draw attention to the occurrence of any problems or changes

92 within the field (inland water, prolonged germination, nutrient deficiency, wildlife damage

93 and plant disease). The development of vegetation can be followed along with the

94 development of NDVI in each field, the effect of different varieties, hybrids, or different crop

4

95   production technologies can be compared. True, these are still not exact values, but they can

96   provide support. In this case, NDVI provides information on the effect of ELICE16INDURES.

97   Using NDVI spectral analysis we monitored the area as indicated in Figure 2A.

98   Photosynthetic traits are indicators of the physiological status of plants. The higher NDVI

99   value suggested a larger area with enhanced photosynthetic activity in leaves of investigated

100 barley culture. This state might have resulted in fewer patients or better assimilation of

101 nutrients, water, or light. We hypothesized that the higher NDVI values correlated with the

102 healthier leaf surface. Therefore we chose plot 8 and plot 1 to highlight the background of

103 this phenomenon. NGS sequencing (GEx) was carried out using plant materials collected in

104 the given plots. We performed bioinformatics analysis and determined the top50 DEGs

105 (Figure 2C).

106

Determination of DEGs in field populations of *H. vulgare*

108   NGS GEx was performed from randomly collected leaves grown in the two parallel

109 plots (see Figure 2). Three biological repeats were investigated in both conditions. Among

110 the top50 DEGs the most interesting genes are detailed in Supplemental Table S1. Results

111 highlighted an outstanding defense response interconnected with JA pathway and oxidative

112 regulation. TIFY 11 –like proteins have a role in response to wounding and JA-mediated

113 immune response. TIFY11 is a member of the family TIFY with a conserved domain taking

114 part in jasmonate signaling. These proteins may be up-regulated by jasmonate, wounding,

115 and herbivores. Chung and Howe report on the critical role of the TIFY motif in repression to

116 JA signaling by a stabilized splice variant of the JASMONATE ZIM-domain protein JAZ10 in *A.*

117 *thaliana* (Chung and Howe, 2009). Our results indicated a strong up-regulation of TIFY11

118 gene after two days of ELICE16INDURES treatment in field conditions. This may suggest that

119 repression of JA pathway was eliminated by TIFY11 protein under ELICE16INDURES

120 conditions, presumably. This result points out the priming-activity of ELICE16INDURES which

121 may be associated with JA pathway regulation. JAZ protein family shares a conserved TIFY

122 motif within the ZIM domain which are key regulators of jasmonate signaling (Thines et al.,

123 2007). Interestingly we found a strong up-regulation of RHOMBOID-like protein 2

124 interconnected with TIFY 11. Rhomboid proteases regulate intramembrane proteolysis

125 recognizing a distortion in a short stretch of amino acids in a transmembrane region

126 (Kanaoka et al., 2005). This function is a fundamental mechanism for controlling a wide

5

127   range of cellular functions. The relationship of rhomboid proteases with JA pathway was

128   described by (Knopf et al., 2012). They report on RHOMBOID function, with chloroplast

129   rhomboids being involved in allene oxide synthase (AOS) accumulation in the *A. thailana*

130   inner envelope membrane which is one of the three key enzymes of the chloroplastic step of

131   JA biosynthesis (Figueiredo et al., 2015). We found that rhomboids were up-regulated in this

132   experiment suggesting that JA metabolism was strengthened at the peroxisome-related step

133   involving up-regulation of peroxidases as well.

134

135   **Testing of ELICE16INDURES in phytotron experiments**

136   Exogenous treatment of SA, BABA, ELICE16INDURES, and their combinations were

137   performed according to the experimental design (Figure 3 A B). Impact on the whole

138   genome expression profiling of ELICE16INDURES was in focus comparing with SA and BABA

139   well studied immune-priming activators. The combination of the investigated three agents

140   resulted in 16 samples, that gene expression comparison was helped by mathematical

141   modeling of most different samples and genes.

142

143   **De novo assembly and mapping**

144   The reference transcript dataset (TrinityH16-transcript, Supplemental Data Set S1)

145   contained 73,301 nucleotide sequences (contigs) that average length was 286 bases with

146   minimum and maximum length 83 and 1,918 bases.

147   All reads from each biological repeat (3 x 16) were separately mapped against the reference

148   dataset one and multiple times. Statistic of mapped reads was performed and compared

149   between all replicates. No significant differences in transcript level and mapping were found

150   between the biological replicates. Therefore reads derived by the same conditions were

151   captured as one sample. The combined read sets were then aligned to the reference

152   containing transcripts. Using this dataset we collapsed unique and common sequence

153   regions among isoforms into a single linear sequence. In our system, this step allows us to

154   analyze the *"in silico poled"* replicates as one sample. If there is a difference in the coverage

155   complexity of a given transcript due to the replication, can be used as average information

156   from the given transcript, representing a gene. The SuperTranscript (assembly at gene level)

157   (TrinityH16-supertranscript, Supplemental Data Set S2) contained 60,614 nucleotide

158   sequences, which were further analyzed.

6

159

Functional annotation

160

Functional annotation of TrinityH16-supertranscript reference dataset was
161 performed. Annotation results are summarized in Supplemental Table S2 that resulted in
162
58.65 % blast results in the NCBI nr database.
163

164

GO categories of the reference transcriptome
165

The entire annotated data set (TrinityH16-supertranscript) indicated an approximate
166 functional distribution of GO term categories. To get the most comprehensive information, 2
167 and 7 levels of categories were taking into account (Supplemental Figure S1). The number
168 and category distribution indicated a high complexity degree of the data set, which allows
169 further GO investigations. Annotation results were used to perform expression comparison
170 during sample-by-sample and gene-by-gene analysis. The high complexity of GO categories
171 correlated with the complexity of reference transcriptome which base the further
172 comparisons of samples involved in this dataset.
173

174

Determination of gene expression profiling in 16 samples
175

The following relations were determined based on count table RPM values: (i) the
176 number of individually expressed genes; (ii) samples having the largest differences in the
177 overall transcription profile; (iii) genes having the greatest changes; (iv) differential
178 expressions of selected samples.
179

180

Individually expressed transcripts
181

Transcripts only expressed in the given sample - were determined based on the count
182 table data. For all 16 samples, 4 x 4 groups were determined to visualize the numerical
183 differences between the expressed genes. The number of common and unique elements of
184 sets are depicted on Venn diagrams (Figure 3). For better understanding grouping was based
185 on the treatment complexity in the 0 and 2 days.
186

From the number of induced genes, results showed that on day 2, the level of gene
187 expression was more significant in the treated samples, except for the ELICE16INDURES +
188 BABA combination treatment, where the number of individually expressed genes decreased
189 by the second day. Based on the control sample, on day 2, the SA stimulus-induced
190

191   alterations in the expression of more than 1000 genes. This trend was also observed by

192   BABA treatments. Combined SA + BABA stimulus may cause a greater change in gene

193   expression than alone. However, this phenomenon showed the opposite in the case of

194   ELICE16INDURES. These samples showed a larger change without SA stimulus. Here, the

195   number of unique transcripts stands out dramatically on day 2. Dual treatment caused fewer

196   transcriptomic changes in each case than the treatments alone.

197

Searching of sample differences by 2-norm

199   We used this method to determine which treatment might cause the largest change

200   in the number of differently expressed genes. Treatment (sample) combinations giving the

201   greatest distances according to the 2-norm were examined. We focused on the outlier

202   values, therefore larger values are marked in green and smaller values in red (Figure 4C).

203   Pink indicates the top 10 combinations (which showed the most larges changes). Based on

204   the distance values in the matrix we selected 2 x 3 samples, which was analyzed in pairwise

205   analysis: (i) 1 vs 10 (ii) 1 vs 11; (iii) 1 vs 13; (iv) 1 vs 15; (v) 1 vs 16; and the outstanding (vi) 9

206   vs 8 combinations. Taking into account the comparison of different effects of treatments

207   alone and in combinations we grouped the pairs into two categories. The direct effect of

208   ELICE16INDURES, BABA, and SA (i-iii) and combined effects of them (iv-vi). Pairwise

209   differential expression analysis with the selected samples was performed. Based on this data

210   the following conclusion might be performed: SA treatment caused the largest change

211   among the investigated materials in the number of expressed genes. Combined treatment

212   such as ELICE16INDURES + BABA + SA at 0 day in comparison with control at day 2 showed

213   large changes in gene expression (8 vs 9). This combined effect was experienced also at day

214   2 such as ELICE16INDURES + BABA and ELICE16INDURES + BABA + SA in comparison with

215   control and SA at day 0 (15 vs 1 and 16 vs 1). SA treatment might strongly affect the gene

216   expression numerically just the day 0 and 2 day as well (10 vs 1, 10 vs 2, 15 vs 2, 16 vs 2).

217   Functional analyzes to determining genes that might be in the background of numerical data

218   were performed (Figure 4B).

219   Sample pairs highlighted with pink showed a high photosynthetic activity associated with

220   chloroplast thylakoid membrane, light-harvesting of photosystems I and II, without

221   exception. This phenomenon showed a strong gene expression measured between days 0

222   and 2. Selected pairs such as (i) 1 vs 10 (ii) 1 vs 11; (iii) 1 vs 13; (iv) 1 vs 15; (v) 1 vs 16; and

223 the outstanding (vi) 9 vs 8 combinations indicated also a strongly enhanced chloroplast
224 activity. Since the enhanced photosynthetic processes were suppressed the other valuable
225 gene expression data, pairwise data was analyzed always on the given day of treatments
226 (Figure 5).

227

228 **Determination of the most variable genes and their functions by 1-norm**

229 Based on distance values according to 1-norm analysis, the top 50 genes showing the
230 most significant changes across 16 treatments were determined and filtered out. These
231 genes showed the highest changes among the samples. An annotation table was assigned to
232 these records. Based on GO terms, we determined biochemical processes that were affected
233 by the top50 genes. The biological process and molecular function of involved genes are
234 summarized in Figure 4A. The screening shows that the genes with the most change in the
235 entire data set are also involved in the biochemistry of the jasmonic acid pathway, which
236 was observed in field experiments as well. Interestingly, pathways responsible for
237 photosynthesis also showed a large change as a result of the treatments, which are
238 consistent with the NDVI studies. The listed oxidation-reduction system, as well as the
239 cadmium ion response associated with oxidative stress, suggested that the antioxidant
240 enzyme system was also stimulated in the samples, which is consistent with previous
241 literature data for salicylic acid and BABA applications (Guo et al., 2013; Pastor et al., 2013).
242 From this study, we determined which biological processes are most affected by the
243 treatments. The up-and down-regulation of these processes was in focus in our further
244 experiments such as the jasmonic acid pathway, (ii) photosynthesis, (iii) cellular respiration,
245 and (iv) regulation of oxidative stress.

246

247 **Pairwise differential expression analysis**

248 To help the selection of sample pairs that were analyzed, we based these
249 comparisons on the differences determined by the 2-norm. Top50 DEGs of the pairs of single
250 treatments on days 0 and 2 were determined using enrichment analysis (Fisher's Exact Test).
251 The DEGs were further performing GO analysis. The GO categories of over-expressed genes
252 are illustrated using WordCloud based on GO IDs Fisher results (Figure 5A-F). These results
253 indicated different mechanisms of action of the three investigated immune-priming agents.

9

254   It can be seen that pathways of pathogen responses involved to priming are induced

255   immediately after BABA addition which was associated with regulation of cellular redox

256   homeostasis. Gene induction effect of BABA-priming decayed on day 2. In contrast, SA

257   showed a prolonged effect on priming genes such as response to external biotic stress to

258   fungus and other organisms was induced strongly on day 2. Genes involved in this process

259   showed high hydrolase, glucosidase, or chitinase activities as described earlier for example in

260   rice by pathogen-derived elicitors and SA (Silverman et al., 1995). We found that

261   ELICE16INDURES enhanced the photosynthesis just after addition, which effect was not

262   observed analyzing SA and BABA treated samples. Enhanced photosynthesis may explain the

263   higher NDVI data observed in field experiments. Mechanism of action of this agent during

264   priming indicated a strong redox activity and high expression of DNA binding transcription

265   factors. The transcription factor regulation through redox changes associated to plant

266   pathogen defense mechanisms were observed for just about 25 years (Wu et al., 1997;

267   Zhang et al., 1999; Dangl and Jones, 2001; Mou et al., 2003; Wendehenne et al., 2014).

268   Transcription regulatory activity corresponded to the high expression of TIFY domain

269   proteins. Further analysis of the ELICE16INDURES application on day 2 was performed

270   making a heatmap and determine the top50 DEGs (Supplemental Figure S2). In this

271   investigation sample 9 (Control of day 2) and sample 13 (ELICE16INDURES of day 2) were set

272   up as test and reference data sets. Gene set enrichment analysis of top50 DEGs obtained

273   from heatmap and GO information are summarized in Supplemental Table S3. We found

274   overexpression of genes of TIFY 3A (TRINITY_DN489_c0_g1, TRINITY_DN966_c0_g1), TIFY 9

275   (TRINITY_DN354_c0_g1),   TIFY   10A   (TRINITY_DN8954_c0_g1),   TIFY   11B

276   (TRINITY_DN299_c0_g1) involving to JA response. *Arabidopsis* TIFY homologs, JAZ proteins

277   act as negative regulators in JA signaling (Chini et al., 2007; Thines et al., 2007; Vanholme et

278   al., 2007), and in response to JA and wounding TIFY domain proteins might be

279   overexpressed. However, in cereal plants, TIFY mediated JA signal may work differently,

280   hypothetically. In rice extensive up-regulation of OsTIFY10 and 11 members, moderated up-

281   regulation of OsTIFY3 and OsTIFY9, and no change in the expression of OsTIFY1a and

282   OsTIFY2a was observed in jasmonate associated growth. TIFY1a and TIFY2a were not

283   differentially changed in our study as well. This was manifested by increased growth, grain

284   weight, and flower number associated with shortened period to flowering. Since rice was

10

285   not sensitive to external jasmonate addition, Hakata et al suggested that TIFY genes may

286   promote growth by desensitizing plants to JA (Hakata et al., 2017). We observed yield

287   increase in field conditions of ELICE16INDURES barley cultures corresponding to the findings

288   of Hakata and al. Enhanced oxidoreductase activity suggested a strong effect of oxidative

289   stress regulation of ELICE16INDURES which was just predicted during field experiments. JA

290   response was mediated primarily by serine-threonine protein kinase signal transduction

291   pathways. This may indicate the mechanism of action of ELICE16INDURES might be

292   associated with receptor signaling of Jasmonate-mediated plant responses.

293

294   **Determination of expression changes of genes of interest (GOIs)**

295   Responses to certain or multiple stress factors are a complex task of plants in which

296   central regulatory hormones such as SA, JA, ethylene, and ABA play key roles. Since the

297   defense mechanisms are complex regulation of these hormones overlapping and linked –

298   positive and negative - regulation may be observed (Ahmed et al., 2013). Many natural-

299   based elicitors may induce a primed state in plants regulating hormonal pathways and

300   modulating antioxidant systems (Aranega-Bou et al., 2014). Taking into account these

301   regulatory pathways we investigated the gene expression changes in samples 1-16 in

302   phytotron experiments. Genes associated with SA, JA, ABA pathways, and redox-system

303   were analyzed *in silico*. Validation of *in silico* gene expressions was performed by RT-qPCR

304   analyses (Figure 6 B-C).

305   In or study 20 genes (GOIs) and their interconnected regulation were investigated

306   involving SA, JA, ABA and AOS genes. Functional analysis of extracted cds was performed

307   before mapping GEx reads. These annotations such as GO terms and enzyme pathway

308   analysis are summarized in Supplemental Table S4. PRD was calculated to analyze how much

309   gene expressions changed relative to themselves. Synergistic and antagonistic effects of

310   exogenous addition of priming-elicitors SA and BABA were investigated and compared with

311   ELICE16INDURES hypothetical priming-active compound.

312

313   **Regulation of SA pathway genes.** The key SA regulators are ICS and PAL which enzymes may

314   help plants in their protection against environmental stresses and are modulated by

315   different abiotic, biotic stress factors and during defense processes (Wildermuth et al.,

316   2001). SA application can positively regulate these enzymes - such as high expression and

317 enhanced activity - during drought, salt, chilling, heat, heavy metal and UV-B radiation

318 stresses(Khan et al., 2015). In barley under drought conditions overexpression of ICS was

319 correlated with a higher activity of antioxidant enzymes and lower levels of reactive oxygen

320 species (Wang et al., 2021). Application of SA enhanced the activity of CAT, peroxidases,

321 SOD, APX, GR under heavy metal stresses in different plant species (Arif et al., 2020). In our

322 results, SA application upregulated ICS2 however repressed PAL by 20%. BABA and

323 ELICE16INDURES treatments acted synergistically with exogenous SA addition to both genes.

324 Correlation with GSH pathway and AOE genes were observed with exogenous SA application

325 except for SOD that was repressed. Since during control conditions SOD was repressed as

326 well, we supposed that SA treatment does not achieve its enhanced effect on the

327 photosynthetic membrane and photosystem II activity involving the antioxidant system.

328 **Regulation of JA pathway genes.** Plant immunity especially involves JA biosynthesis and

329 signaling in plant defenses against necrotrophic and insect infections (Brenya et al., 2020).

330 During JA biosynthesis the chloroplast and the peroxisome are participating therefore

331 lipoxygenase activity may play a key role in JA-induced priming. We detected enhanced LOX3

332 activity in all treatments suggesting a positive effect on the JA pathway. A similar effect was

333 proved in the case of Vitamin B2 (Azami-Sardooei et al., 2010; Taheri and Tarighi, 2010).

334 Furthermore, high AOC up-regulation was detected by BABA that could act synergistically

335 with SA and ELICE16INDURES. Contemporarily BABA represses OPR3 in opposite with SA and

336 ELICE16INDURES. Since OPR3 catalysis dnOPDSA to OPC6 step in peroxisomes, this suggests

337 the effect of BABA may be concentrated in chloroplast-joint scenarios or Beta-oxidation in

338 peroxisomes (Ruan et al., 2019). BABA showed a high effect acting antagonistically on the

339 other two investigated materials. Based on the results of field experiments TIFY11 and

340 RHOMBOID-like protein 2 were also analyzed in these samples. Time course positive

341 regulation of TIFY11 and RHOMBOID-like protein 2 genes were observed in phytotron

342 experiments in correspondence with field investigations. This phenomenon was detected in

343 the case of ELICE16INDURES and combined treatment with BABA. However single BABA and

344 SA treatments didn't regulate these genes outstandingly. Transcriptional control of the JA

345 pathway may be controlled by several factors (Caarls et al., 2015), therefore positive or

346 negative gene regulation by different inducers is not surprising. Our results suggest that

347 BABA and ELICE16INDURES induced outstanding changes in the JA-signaling, in contrast with

348 SA which had less effect on these genes.

349 **Regulation of ABA pathway genes.** The accumulation of ABA is controlled by the enzyme 9-

350 cis-epoxycarotenoid dioxygenase (NCED). Strong negative regulation of NCED1 by all

351 treatments was found in this experiment. NCED1 was significantly down-regulated in

352 drought stress, at which time ABA content reached a peak (Liu et al., 2016). However

353 negative regulation of NCED1 is unclear and little studied. Our results indicated that plant

354 responses to the investigated immune-priming activators might be manifested in the

355 negative feedback of NCED1.

356 **Regulation of GSH metabolism genes.** The expression of antioxidant enzyme genes under

357 different stresses was tested in a few studies on barley (Harb et al., 2015) which detail that

358 abiotic and biotic stresses strongly induces expression of these genes promoting

359 detoxification. We investigated how these genes may be altered to exogenous metabolic

360 enhancers which may be associated with priming. BABA, SA and ELICE16INDURES synergistic

361 and antagonistic effects on the regulation of GSH pathway and AOS were therefore

362 analyzed. In plants, glutathione (GSH) metabolism is a key part of AOS and stress

363 management. It is required for efficient defense against plant pathogens. Many enzymes use

364 GSH as an electron donor or as a substrate during sulfur assimilation, flower development,

365 salicylic acid, and plant defense signaling. We investigated the PRD values of GSH pathway

366 key genes such as ascorbate peroxidase (APX), dehydroascorbate reductase (DHAR), GSH

367 peroxidase (GPX), GSH reductase (GR) and GSH synthase (GSS).

368 GSS is the second enzyme in the GSH biosynthesis pathway. It catalysis the condensation of

369 gamma-glutamylcysteine and glycine, to form glutathione. In *A. thaliana* low levels of GSS

370 have resulted in increased vulnerability to stressors such as heavy metals and toxic organic

371 chemicals (Maksymiec et al., 2005). The presence of a thiol functional group allows its

372 product GSH to serve both as an effective oxidizing and reducing agent in numerous

373 biological scenarios (Saez et al., 1990). GSS was changed negatively only in the case of SA

374 treatment, other treatments did not affect this gene.

375 In plants, GR catalyzes the reduction of GSH disulfide (GSSG) to the sulfhydryl form GSH,

376 which is a critical molecule in resisting oxidative stress and maintaining the reducing

377 environment of the cell. It is part of the glutathione-ascorbate cycle in which reduced GSH

378 reduces dehydroascorbate, a reactive byproduct of the reduction of hydrogen peroxide. In

379 particular, GR contributes to plants' response to abiotic stress. The activity of enzymes was

380 modulated in response to metals, metalloids, salinity, drought, UV radiation, and heat-

13

381   induced stress (Gill et al., 2013). A strong up-regulation in GR expression was detected after

382   BABA treatment and down-regulation after SA treatment. Exogenous addition of SA and

383   ELICE16INDURES may impair the BABA effect. However, the synergistic effect on GR up-

384   regulation was observed in the case of SA + ELICE16INDURES combination.

385   GPXs enzyme family possesses nine stress-related genes with conserved domain and high

386   homology in plant species. These enzymes reduce lipid hydroperoxides to their

387   corresponding alcohols and reduce free hydrogen peroxide to water. GPXs are induced by

388   oxidative stress (Khan et al., 2020) pathogen infections (Pieczul et al., 2020), mechanical

389   stimulation (Singh et al., 2020), salt, cold, drought and metal treatments (Han et al., 2020).

390   DHAR regulates the cellular ascorbic acid redox state, which in turn affects cell

391   responsiveness and tolerance to environmental ROS. DHAR is important for plant growth

392   such as maintain steady-state chlorophyll and Rubisco (Chen and Gallie, 2006). Upregulation

393   of GPX and DHAR was observed in all treatments except ELICE16INDURES.

394   APX is part of the ascorbate–glutathione cycle, which requires ascorbate to scavenge H_2O_2

395   (Reddy et al., 2004; Sousa et al., 2015). APX was regulated negatively by ELICE16INDURES

396   which effect may be slightly observed in the combined treatments (ELICE16INDURES + BABA

397   + SA, ELICE16INDURES + BABA). A synergistic effect on the APX up-regulation was observed

398   in BABA + SA combined treatment.

399   To summarize, GSH metabolism may be accelerated by the investigated priming-

400   active substances, among which the most effective was the BABA treatment. This effect is

401   outstanding in the case of GR. The other two substances show higher activity in combination

402   suggesting synergistic effects.

403

404   **Validation of enhanced expression of TIFY family members and RHOMBOID like protein 2**

405   The role of TIFY-motif proteins in JA signaling is known (Chung and Howe, 2009) however

406   which stress factors may activate the TIFY-mediated events is less studied. In this study

407   applying a comprehensive genome-wide bioinformatics analysis, we experienced that JA

408   response was strongly associated with thylakoid membrane scenarios at the gene expression

409   level. This phenomenon was remarkable triggering priming-associated genes by

410   ELICE16INDURES. The expression profile performed by *in silico* predictions was validated by

411   the RT-qPCR technique using plants cultivated in the phytotron. TIFY3A, TIFY9, TIFY10A,

412   TIFY11B and RHOMBOID-like protein 2 showed a strong up-regulation after ELICE16INDURES

14

413   treatment at day 2. Expression of these genes was observed after BABA and SA treatment at

414   a significantly lower rate. TIFY3A was downregulated by SA. All substances triggered the

415   relative expression of the RHOMBOID protein. Since rhomboid proteins are proved to be

416   associated with the internal region of the thylakoid membrane we concluded that

417   ELICE16INDURES possess a priming effect through JA signaling. This hormonal regulation

418   takes place in the chloroplast. Since we observed augmented photosynthetic areas in field

419   experiments meaning an increased amount of chloroplasts in ELICE16INDURES treated plots,

420   we concluded that higher gene levels of JA pathway genes (AOC, LOX, OPR1) correlated also

421   with enhanced TIFY and Rhomboid proteins in phytotron experimental setup (Figure 6 A-C).

422   The role of chloroplast-Rhomboid proteases was studied in *A. thaliana* indicating to have a

423   positive impact on fertility and flowering through JA signaling (Adam, 2015)

424   Plant immune response may be interconnected by various metabolic pathways, among

425   which the most important is the photosynthetic activity from farming aspects. Alterations in

426   physiological chloroplast events lead to plant wilting therefore understanding chloroplast

427   function associated with priming is considerable. Since chloroplast is a major synthesis site

428   for many plant hormones such as ABA, JA, SA, and free radical production, there is a complex

429   relationship between photosynthesis and defense-related signals (Lu and Yao, 2018) which

430   scenarios take place in thylakoid membranes, primarily. The rhomboid family of serine

431   proteases plays a pivotal role in a diverse range of pathways, activating and releasing

432   proteins via thylakoid intramembranous proteolysis. The plastid intramembranous

433   proteolysis of RHOMBOIDs was studied in *A. thaliana* and found that the lack of chloroplast-

434   located rhomboid proteases caused reduced fertility and aberrations in flower morphology

435   which was interconnected to JA signaling (Adam, 2015).

436

437   **MATERIALS AND METHODS**

438   **Priming-active compounds**

439   ELICE16INDURES was produced in the Institute of Medicinal Plant and Herbs, Ltd, Hungary.

440   We used the high-pressure extraction with supercritical carbon dioxide as a solvent ($scCO_2$

441   extraction). 11 $scCO_2$ extracts of medicinal plants were establishes in a common set of states

442   and encapsulated in sunflower lecithin based liposomes (Figure 1 D). The ratio of $scCO_2$

443   extracts see in Figure 1B. We reach to entrap the active agents into small multilamellar

444   vesicles (MLV) of 250-350 nm by using active trapping techniques (Mayer et al., 1986).

445 Transmission electron microscopy (TEM) was used to characterize the sizes and structures of

446 liposomes in the range 10-1000 nm. Liposome structures were visualized and analyzed by

447 TEM (Figure 1). Active compounds of ELICE16INDURES are summarized in Supplemental

448 Table S5. scCO$_2$ extracts were purchased from FLAVEX Naturextrakte GmbH, Germany. The

449 two immune priming activator compounds SA and BABA (purity 99 and 97%) were

450 purchased from Merck (MilliporeSigma, US).

451

TEM processing and particle size analysis

453 Samples for transmission electron microscopy (TEM) were prepared by diluting liposome

454 concentrates with MQ water and depositing a drop of the suspension on copper TEM grids

455 covered by continuous carbon amorphous support film. After 5 minutes the drop was

456 blotted with filter paper. Diluted (2%) phosphotungstic acid was used for sample staining.

457 The staining time was 30 seconds. Measurement conditions were as follows: TEM analyses

458 were performed using a Talos F200X G2 instrument (Thermo Fisher), operated at 200 kV

459 accelerating voltage, equipped with a field-emission gun and a 4096x4096 CMOS camera for

460 imaging. In our study TEM bright-field images were collected at 36000x magnification for

461 particle size analysis and other magnifications as well to visualize the details and the inner

462 structures of the liposomes.

463 Particle size analysis was performed based on TEM bright-field images using Gimp and

464 ImageJ software. The Gimp software was used for image processing (including contrast

465 enhancement, blurring, and manual outlining) and ImageJ was used for creating the final

466 image with grayscale threshold settings and for an analysis of particle sizes. The smaller

467 particles had continuous borders and sufficient contrast for distinguishing them from their

468 background with proper threshold settings, enabling ImageJ to recognize these particles. We

469 could not use this method directly on the larger particles because of their diffuse details or

470 discontinuous borders. Therefore, we manually outlined and filled the larger particles with

471 black color to create an image with white background and black particles. As the last step,

472 we removed the black pixels forming bridges between the particles to create the final image

473 for the particle size analysis.

474

Cultivation of plant materials and chemical treatment

16

476 Fresh leaves were collected on days 0 and 2 after treatments from 11-16-day-old autumn

477 barley plants (diploid). Day 0 means 2-3 hours after treatment. Plants were cultivated in

478 phytotron and arable fields.

479 **Phytotron experiments**. Exogenous treatment of SA, BABA, and ELICE16INDURES was

480 performed in phytotron experiments. Plant growth chamber type was MLR352HPA -115V

481 NEMA 5-20, 220V / 60Hz – Panasonic. Treatment conditions were as follows: temperature

482 during the 1. day and night was 25 °C. The temperature during the 2-16. days and nights

483 were 25 °C and 15 °C. Duration of the day was 12 hours, 04-4 p.m. Treatments were as

484 follows: Na-SA (MW: 160.11 g/mol), 300 µM- solution; BABA (MW: 103.121 g/mol), final

485 concentration in soil was 25 µM; ELICE16INDURES, 1 ml/100ml water. Experimental design

486 and sample collection were performed according to Figure 3A and B.

487 **Field experiments.** Plants in field experiments were sprayed by TTAM4E drone with low and

488 high doses of ELICE16INDURES. We used a positive control that was a commercially

489 available plant conditioner, Fitokondi®. Applied doses and plot allocations were: 1, control

490 without treatment; 2, positive control treated with Fitokondi; 3, 10 g/ha; 4, 20 g/ha; 5, 30

491 g/ha; 6, 60 g/ha; 7, 120 g/ha ; 8, 240 g/ha ELICE16INDURES. Plot allocation of doses see in

492 Figure 2A. After sample collections, samples were prepared for RNA-sequencing and gene

493 expression profiling. Three biological repeats were investigated.

494

495 **Determination of normalized difference vegetation index (NDVI) by remote sensing**

496 To monitor NDVI in the field population we used a DJI-phantom 4 agro drone equipped with

497 a near-infrared camera. The recording was carried out on day 2 after treatment. Single aerial

498 pictures were combined afterward with AgiSoft Photoscan Professional software using high-

499 quality dense cloud processing and mesh construction settings (Figure 2A). To NDVI

500 calculation after identifying the plots based on combined aerial photographs, sample areas

501 were cut out using self-developed software. Sample collection for molecular biological

502 analysis was performed at the same day.

503

504 **Preparation of RNA-seq libraries**

505 Approximately 30 mg of plant tissues were placed in a 1.5 ml Eppendorf LoBind tube

506 containing glass beads (1.7-2.1 mm diameter, Carl Roth, Karlsruhe, Germany) and 100 µl of

507 TRI-Reagent (Zymo Research). The Eppendorf tube was firmly attached to a SILAMAT S5

17

508 vibrator (Ivoclar Vivadent, Schaan, Liechtenstein) to disrupt and homogenize the tissue for

509 2x15s. Total RNA was extracted using Direct-zol™ RNA MiniPrep System (Zymo Research)

510 according to the manufacturer's protocol. The RNA Integrity Numbers and RNA

511 concentration were determined by RNA ScreenTape system with 2200 Tapestation (Agilent

512 Technologies, Santa Clara, CA, USA) and RNA HS Assay Kit with Qubit 3.0 Fluorometer

513 (Thermo Fisher Scientific, Waltham, MA, USA), respectively. For Gene Expression Profiling

514 (GEx) library construction, QuantSeq 3' mRNA-Seq Library Prep Kit FWD for Illumina

515 (Lexogen GmbH, Wien, Austria) was applied according to the manufacturer's protocol. The

516 quality and quantity of the library were determined by using High Sensitivity DNA1000

517 ScreenTape system with 2200 Tapestation (Agilent Technologies, Santa Clara, CA, USA) and

518 dsDNA HS Assay Kit with Qubit 3.0 Fluorometer (Thermo Fisher Scientific, Waltham, MA,

519 USA), respectively. Pooled libraries were diluted to 1.8 pM for 1x86 bp single-end

520 sequencing with 75-cycle High Output v2 Kit on the NextSeq 550 Sequencing System

521 (Illumina, San Diego, CA, USA) according to the manufacturer's protocol. By using longer

522 reads QuantSeq FWD allows to exactly pinpoint the 3' end of poly(A) RNA and therefore

523 obtain accurate information about the 3' UTR. Using this sequencing fragments of coding

524 sequences are 260-300 bp long on average.

525

Bioinformatics analysis – reads processing

527 3 x 16 libraries were sequenced with a final output single-end, 15-18 M x 80 bases long.

528 Quality control (QC), trimming, and filtering of .fastq files were performed in preprocessing

529 step. The QC analysis was performed with FastQC (Andrews et al., 2010) software. For all the

530 3 x 16 libraries the Phred-like quality scores (Qscores) were set to >30. Poor quality reads,

531 adapters at the ends of reads, limited skewing at the ends of reads were eliminated by using

532 Trimmomatic (Bolger et al., 2014). Contamination sequences and N's were filtered out with a

533 self-developed application GenoUtils as described earlier (Mátyás et al., 2019): reads

534 containing N's more than 30 % were eliminated; reads with lower N' ratio were trimmed

535 with a final length > 65. Reads passed of preprocessing were further assembled and

536 analyzed.

537

***De novo* assembly and mapping**

539 Reference transcript dataset was firstly created from the libraries (TrinityH16-transcript,

18

540   Supplemetal File S1). To increase the coverage of the transcripts *de novo* assembly was

541   performed with all the cleaned reads of combined 3 x 16 libraries. To obtain longer mRNA

542   fragments from the combined short reads (65-80bp) without reference Trinity assembler

543   with 23K-mer were used (Grabherr et al., 2011). For *de novo* assembly and mapping we used

544   a server with 512 GB (Gigabytes) of RAM, 64 cores (CPUs), and Ubuntu as the operating

545   system. To assess the read composition of the assembly, input RNA-Seq reads were aligned

546   to the transcriptome assembly using Bowtie2 (Langmead and Salzberg, 2012). All reads from

547   each biological repeat (3 x 16) were separately mapped against the reference dataset. Reads

548   mapped to the assembled transcript were captured. Statistic of mapped reads was

549   performed and compared between all replicates. We used TrinityH16-transcript for gene

550   expression profiling. Collapsing of splicing isoforms were performed with OmicsBox and

551   SuperTranscripts (gene-level assembly) were used in further investigations TrinityH16-

552   supertranscript, Supplemental Data Set S2. Trinity H-field (Supplemental Data Set S6)

553   transcript dataset of filed experiments were performed with the same method.

554

555   **Gene level quantification**

556   To estimate gene expression from RNA-sequencing CountTable was created (Supplemental

557   Data Set S3). To count how many reads map to each feature of interest (transcripts) each

558   sample reads were aligned to the reference TrinityH16-supertranscript. Count Table creation

559   was performed with omixbox.biobam (OmicsBox, https://www.biobam.com/omicsbox)

560   using the HTseq package (Anders et al., 2015). Based on the data of CountTable further

561   analyses were performed such as differential expression analysis and mathematical

562   prediction of the test area.

563

564   **Pairwise differential expression analysis**

565   Numerical analysis of differentially expressed genes (DEGs) in a pairwise comparison of two

566   different experimental conditions - *gene expression analysis* – was carried out using

567   omixbox.biobam (OmicsBox, https://www.biobam.com/omicsbox). The used application is

568   based on the edgeR program implementing quantitative statistical methods to evaluate the

569   significance of individual genes between two experimental conditions (Robinson et al.,

570   2010). TMM (Weighted trimmed mean of M-values) normalization method was performed.

571

19

Functional annotation

Functional annotation and Gene Ontology (GO) analysis were carried out using OmixBox.Biobam as follows: 1. Sequences were blasted against NCBI nr (non-redundant) Viridiplantae database (downloaded in 2019) applying blastn configuration locally; 2. To retrieving GO terms associated with the 10 Hits obtained by the Blast search GO mapping and annotation were performed. GeneBank identifiers (gi), the primary blast Hit ids, were used to retrieve UniProt IDs making use of a mapping file from PIR (Non-redundant Reference Protein Database) including PSD, UniProt, Swiss-Prot, TrEMBL, RefSeq, GenPept and PDB. Accessions were searched directly in the dbxref table of the GO database. BLAST result accessions were searched directly in the gene-product table of the GO database; 3. GO annotations were specified according to GO terms: molecular function, cellular component, biological process.

Determination of uniquely expressed transcripts

Count table data of each biological replicates were used. According to the mapping statistics, there were no significant differences between the biological replicates. Average values of counts were taken into account used to create a 60,615 (number of genes, rows) x 16 (number of samples, column) matrix from the count table. Normalization of mapped read counts, RPM index (reads per million mapped reads, Figure 7A) were firstly calculated from matrix data for the determination of uniquely expressed transcripts and mathematical modeling of interest area (see below). Highly characteristic transcripts that were uniquely expressed were filtered out from the matrix with Microsoft access database manager. Identifiers of these transcripts in each treatment condition (sample) were separated and saved in txt files. To the better evaluation graphical representation of results was grouped into 4 Venn diagrams (Figure 3 C-F) using the web-based interactivenn.net (Heberle et al., 2015).

Enrichment analysis

To determine cellular responses and cell-biochemical processes altered between 2 samples and how they are affected by the treatments, Fisher's Exact Test was used. Fisher's Exact Test performs functional analysis of differential expressed genes working with the entire annotated data set previously determined (Huang et al., 2009).

20

604

Mathematical prediction of investigated area examination

606   To predict which treatment conditions show the most different transcriptomic events,

607   search and determination the extremal points of the 16 transcriptome data sets as a

608   multidimensional space. The 60,615 x 16 matrix was analyzed by column and by rows which

609   fields contained the RPM indexes.

610

Searching of sample differences by 2-norm

612   2-norm is a functional on vector space that assigns a non-negative (real) number to the

613   elements of vector space. Hölder norms (e.g., 1-norm, 2-norm, p-norm) can be used to

614   manage distances (length) in abstract spaces. In our case, we took a 60,615-dimensional

615   vector space (with its 16 vectors, Figure 7C), in which the column vectors were spaced. We

616   wondered how far apart these vectors in pairs are. Since the distance function is

617   commutative, therefore in a given comparison, only the two different vectors were counted,

618   their order was not. The examination number was given by a combination of 16 elements

619   without second class repetition which is 16 * 15/2. The distance of 2 columns was given by

620   the value of the vector of the difference between the two vectors according to norm 2

621   (Figure 7 B, C).

622

Searching of differences between genes by 1-norm

624   During this method transcripts showing the largest changes in RPM across the 16 samples

625   were determined. For this analysis, all 60,615 transcripts were involved. For each transcripts,

626   absolute values of the difference in RPM values between the sample pairs were calculated

627   and these values were summarized. We assumed that higher values are stronger in

628   expression. As a result of the analysis, the top 50 genes were determined (Figure 7D).

629

Determination of the most variable cell-biochemical pathways

631   The top 50 transcripts based on distance values by 1-norm were categorized according to GO

632   terms. Cell biochemical processes were examined in more detail. Changes in cell responses

633   as a result of treatment were grouped based on enrichment analysis (Huang et al., 2009).

634

Determination of expression changes of genes of interest (GOIs)

636   We identified the accurate coding sequences (cds) of investigated pathway genes in our

637   plant material. Therefore we used a transcriptome dataset from deep sequencing of three,

638   treated and control phytotron samples of *H. vulgare* (TrinityH-Deep, Supplemental Data Set

639   S4). Sequencing protocol and assembly were used as described earlier (Virág et al., 2016).

640   We identified cds of 20 genes of interest (Supplemental Data Set S5). JA, ABA, SA and GSH

641   pathway genes were determined. Contigs of these genes were identified based on *Oriza*

642   *sativa* and *H. vulgare* using BLASTn with an E value less than 10^{-5} (Altschul et al., 1990). ORF

643   (open reading frame) was determined with NCBI ORF finder. These cds were used as

644   reference sequences to mapping reads of GEx libraries to determine gene expression

645   changes. Time course RPM changes (PRD, percentage of relative difference) as a response to

646   treatments were calculated (formula see in Figure 7E). Expression changes were calculated

647   mapping reads of QuantSeq 3' mRNA-Seq libraries in which one fragment per transcrinpt

648   was produced, therefore, no length normalization was required. This method allows a more

649   accurate determination of expression values in gene expression studies.

650

651   **Gene expression analysis with RT-qPCR amplification**

652   RT-qPCR experiment of GOIs was performed as described earlier (Mátyás et al., 2019).

653   Primers were designed with Primer3 (Koressaar and Remm, 2007; Untergasser et al., 2012)

654   based on *in silico* sequences of GEx libraries. Gene expression analysis was established based

655   on three technical and biological replicates and normalized with the reference gene

656   glyceraldehyde-3-phosphate dehydrogenase, *GAPDH*.

657

658   **Accession Numbers**

659   Raw reads of this project used for field and phytotron experiments (21 SRA experiments) are

660   deposited in the NCBI SRA database under the accessions: Bioproject, PRJNA721578; Deep

661   RNA sequencing, SRX10603947- SRX10603949; Sequencing of field experiments,

662   SRX10598683, SRX10598684; Sequencing of phytotron experiments, SRX10600133-

663   SRX10600148.

664

665   **Supplemental data**

666   **Supplemental Table S1** Annotation of most interesting genes from the top50 DEGs in field

667   experiments.

22

668   **Supplemental Table S2** Results of functional annotation of TrinityH16-supertranscript –

669   reference- transcript dataset.

670   **Supplemental Table S3** Annotation of top50 DEGs of pairwise comparison

671   **Supplemental Table S4** Gene ontology and enzyme annotation of investigated sequences of

672   SA, JA, ABA and GSH pathway genes.

673   **Supplemental Table S5** Biologically active components of ELICE16INDURES.

674   **Supplemental Figure S1** The top20 GO term categories of the reference transcriptome

675   **Supplemental Figure S2** Heatmap of the investigated 16 H. vulgare samples

676   **Supplemental Data Set S1** TrinityH16-transcript.fasta

677   **Supplemental Data Set S2** TrinityH16-supertranscript.fasta

678   **Supplemental Data Set S3** Count Table

679   **Supplemental Data Set S4** TrinityH-Deep

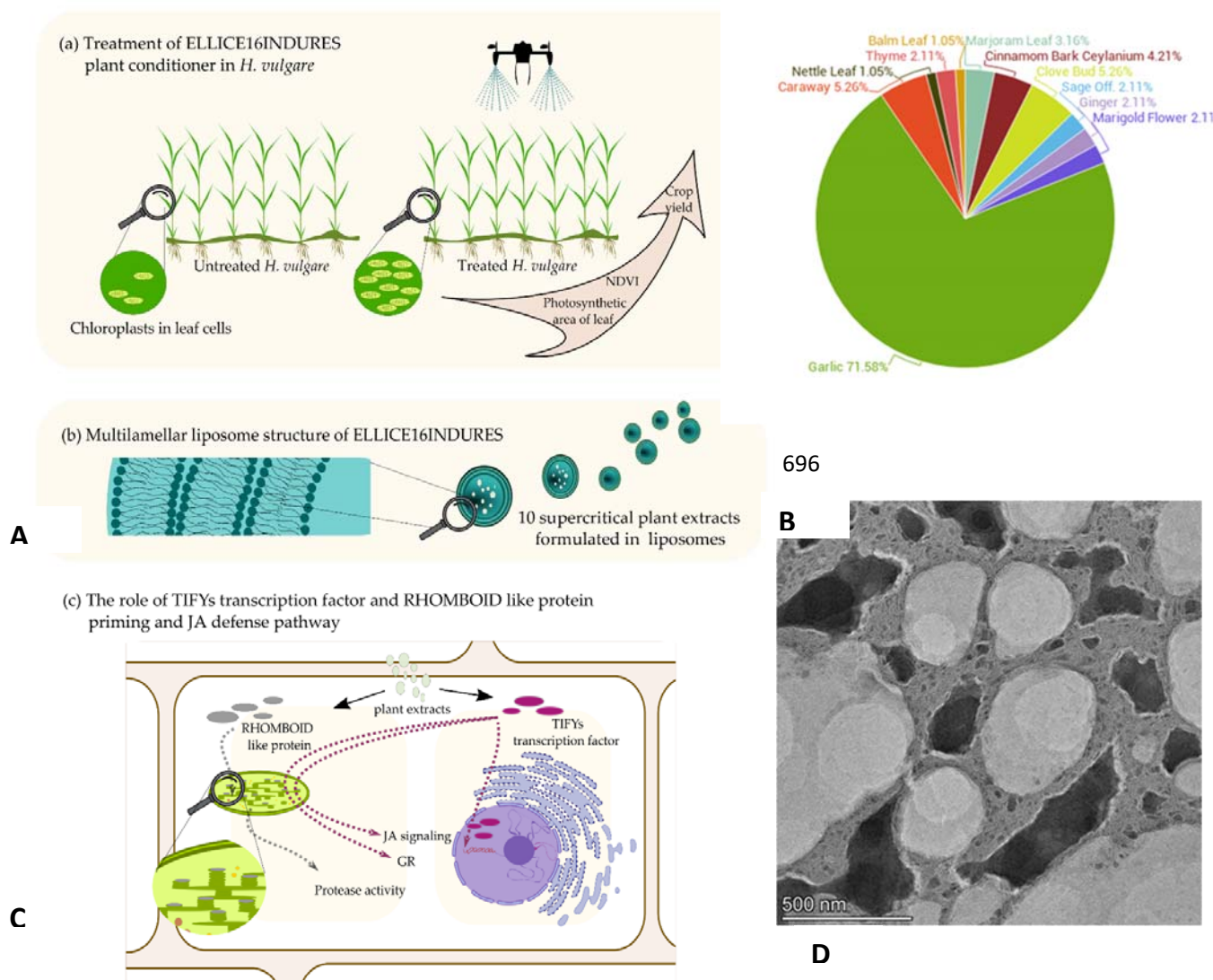680   **Supplemental Data Set S5** Coding sequences and primers GOIs

681

682   **ACKNOWLEDGMENTS**
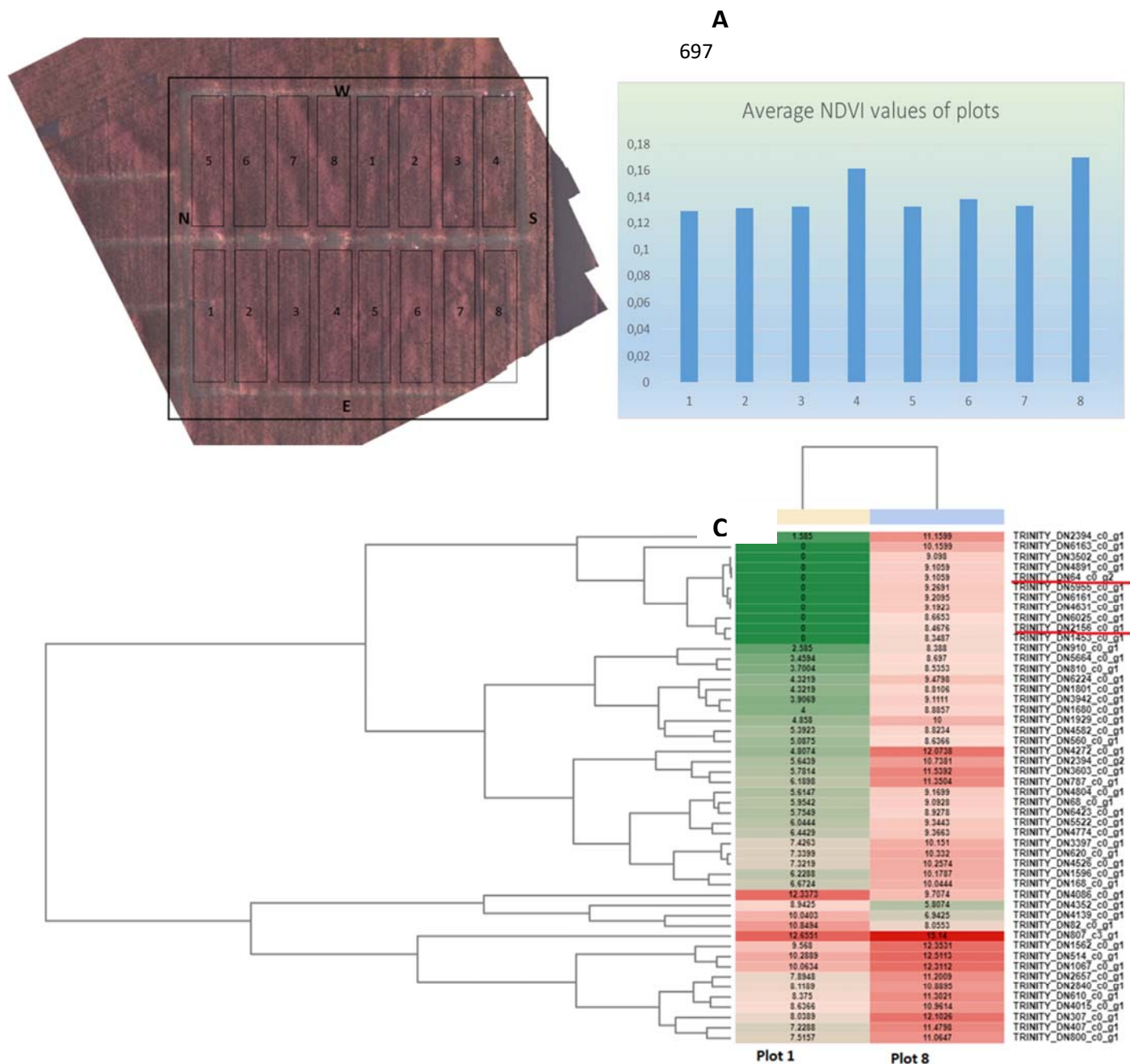
689

690   **AUTHOR CONTRIBUTIONS:** E.V., and J.P.P., designed the project; G.H., M.K., B.L., L.G., Á.N.,

691   P.P., Z.T., performed experiments; K.D., B.K., K. S., E.V., and G.H., analyzed the data., E.V.,

692   and G.H., performed bioinformatics analyses., E.V., and Á.J., wrote the paper.

693

694   **Competing   interests:**   Authors   declare   no   competing   interests.

695

Figures

A

(a) Treatment of ELLICE16INDURES plant conditioner in *H. vulgare*

Untreated *H. vulgare* Treated *H. vulgare*

Chloroplasts in leaf cells

Crop yield
NDVI
Photosynthetic area of leaf

(b) Multilamellar liposome structure of ELLICE16INDURES

10 supercritical plant extracts formulated in liposomes

B

Balm Leaf 1.05% Marjoram Leaf 3.16%
Thyme 2.11% Cinnamom Bark Ceylanium 4.21%
Nettle Leaf 1.05% Clove Bud 5.26%
Caraway 5.26% Sage Off. 2.11%
Ginger 2.11%
Marigold Flower 2.11

Garlic 71.58%

696

C

(c) The role of TIFYs transcription factor and RHOMBOID like protein priming and JA defense pathway

plant extracts

RHOMBOID like protein
TIFYs transcription factor

JA signaling
GR
Protease activity

D

500 nm

E

24

A

697

Figure 2. Field experiments of ELICE16INDURES® on autumn barley cultures

Plots and doses of ELICE16INDURES® applied in field experiments: **1**, control without treatment; **2**, positive control treated with Fitokondi®; **3**, 10 g/ha; **4**, 20 g/ha; **5**, 30 g/ha; **6**, 60 g/ha; **7**, 120 g/ha ; **8**, 240 g/ha ELICE16INDURES®. Experimental areas are visualized by a combined photograph from drone photos **(A)**. A near-infrared camera was used to calculate NDVI from each pixel. The average NDVI of plots calculated from pixel values is visualized on figure **(B)**. Heatmap of top 50 DEGs of *H. vulgare* treated by ELICE16INDURES® in the field **(C)**. Samples were collected randomly from the plot **8** and **1**. Genes highlighted with red are involved in JA-pathway: TRINITY_DN64_c0_g2, protein TIFY 11e-like and TRINITY_DN2156_c0_g1, RHOMBOID-like protein 2. Annotation of heat map see in Supplemental Table S2.
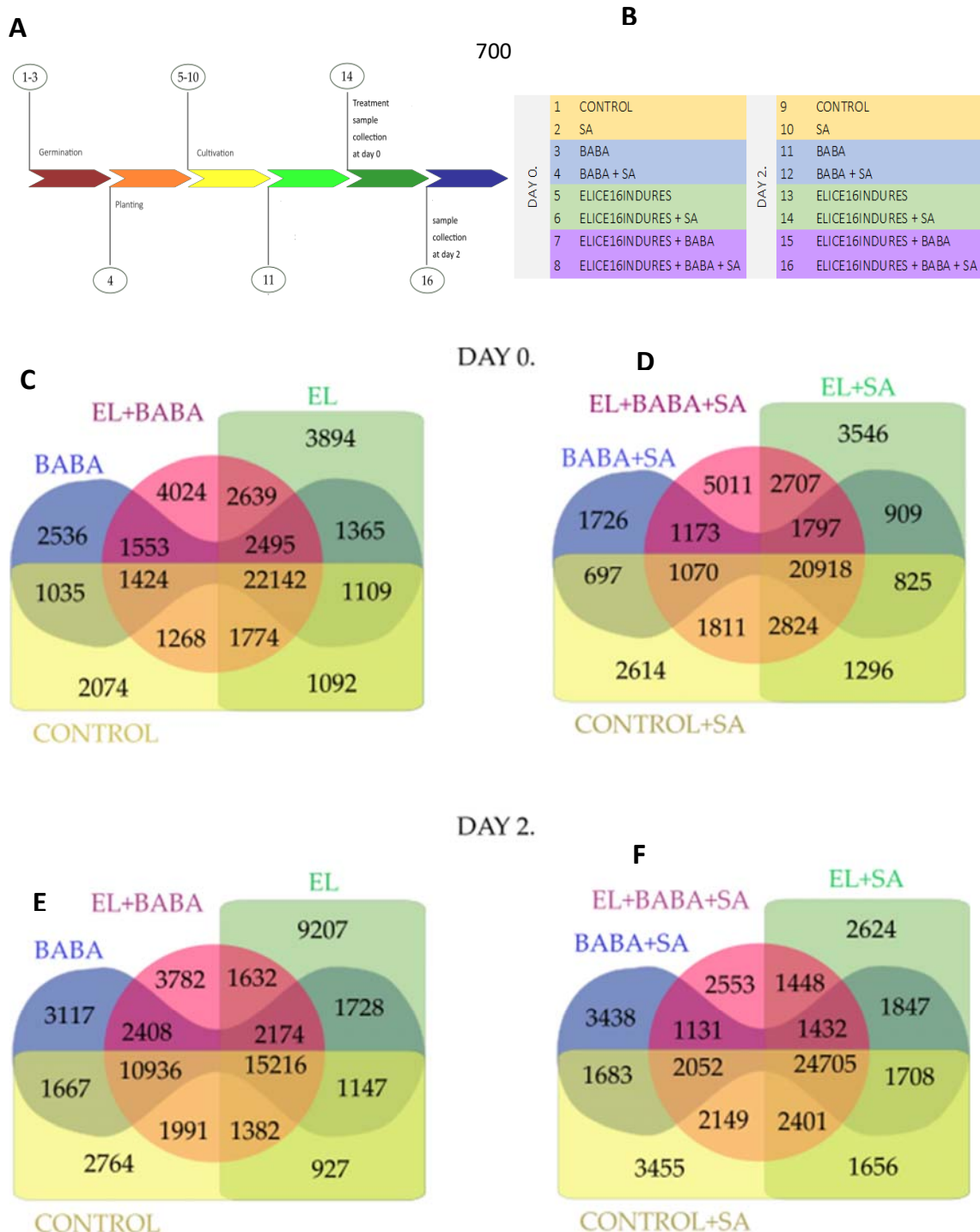
Figure 3. Venn diagrams. Numerical analysis of individually and commonly expressed genes in *H. vulgare* treated by priming-active materials.

Experimental design of phytotron experiments **A** and **B**. Abbreviations: EL, ELICE16INDURES; SA, salicylic acid; BABA, beta-amino butyric acid. Treatments of priming inducing agents were performed on day 14. Sample collections were performed at day 14 **(Day 0)** at day 16 **(Day 2)**.

Samples were collected at day 0 **(C, D)** and 2 **(E, F)** after treatments. Control samples were not treated, these were cultivated under the same conditions as the treated samples. For all 16 samples, 4 x 4 groups were determined to visualize the numerical differences between the expressed genes. **C** and **E** diagrams compare numerically the genes expressed in the case of El and BABA treatments and their combinations. **D** and **F** diagrams compare numerically the genes expressed between the treatments EL and BABA supplemented with SA.

A

Biological processes

ATP Synthesis coupled proton transport
carbon fixation
carbon utilization
dephosphorylation
glucose metabolic process
mitochondrial translation
oxidation-reduction process
photosynthesis light harvesting
photosynthesis light harvesting in photosystem I
photosynthesis, light reaction
photosynthesis
photosynthetic electron transport in photosystem II
photosystem I stabilization
protein stabilization
protein-chromophore linkage
reductive pentose-phosphate cycle
respiratory electron transport chain
response to cadmium ion
response to herbicide
response to jasmonic acid
response to light stimulus
ribosome assembly

Molecular function

acid phosphatase activity
chlorophyll binding
electron transporter, transferring electrons within cytochrome b6/f complex of photosystem I activity
glutamate-ammonia ligase activity
rRNA binding, structural constituent of ribosome, zinc ion binding
linoleate 13-S-lipoxygenase activity
lyase activity
NAD binding
NADH dehydrogenase (ubiquinone) activity
oxydoreductase activity, acting on the aldehyde or oxo group of donors, NAD or NADP as acceptor
phosphate ion binding
RNA binding
electron transporter, transferring electrons within the cyclic electron transport pathway of photosynthesis activity
ribulose-bisphosphate carboxylase activity

B

C

Figure 4. Searching of sample differences by 2-norm and determination of most variable genes by 1-norm

Cell biochemical processes and molecular function of the top50 gene showing the largest change in the total data set of 16 samples determined by 1-norm are visualized (**A**).

Column combinations (16 x 15/2) in sample difference searching process by 2-norm (**C**). Numbers means the treatments according to experimental design. Pink-colored values are the top 10 sample combinations with the highest expression differences. Columns showing the greatest differences for the total transcriptomic data may determine which two samples had the largest difference in gene expression at the total gene level; namely which 2 samples have the most different transcriptomic pattern. Values indicate the distances between the samples. A higher value means more different patterns. Sample pairs selected based on the table were used to perform pairwise gene expression analysis. To better understanding, a WordCloud (**B**) of gene set enrichment analysis of sample pairs screened with 2-norm was performed. Words mean GO categories of pink-colored values that were highlighted in

	1	2	3	4	5	6	7	8	9	10	11	12	13	14	15	16
1		15063,52	19009,75	38650,36	52863,75	40330,02	31661,76	31177,43	107752,2	89594,25	64914,28	40226,72	51883,36	71400,96	95612,85	96149,21
2			31506,78	50710,08	62574,11	49011,43	40095,36	37282,8	118005,2	100568,9	76678,51	50037,57	62920,75	82629,32	107234,6	107845,7
3				25272,27	41347,17	32317,08	24770,74	28070,78	94596,91	75443,84	50044,72	29458,06	39113,25	57600,95	80617,14	81140,68
4					28341,85	24550,29	25548,67	31930,51	76470,02	57639,57	34325,73	24130,76	28148,54	42550,75	63898,69	64347,78
5						16932,28	23278,19	28451,62	56816,72	39522,95	28122,53	21593,88	16618,2	26134,2	49287,61	50133,2
6							11690,21	15522,43	70009,04	53842,17	39207,4	19219,68	23535,98	38610,34	63390,46	64025,41
7								8151,309	78701,92	61568,97	43025,94	18301,39	26747,37	44878,23	69876,37	70502,49
8									83086,85	66631,66	48946,62	22576,7	32142,63	50035,71	75170,71	75865,54
9										25022,9	57778,21	74485,15	61942,81	44899,72	35973,68	36498,77
10											34338,84	53916,91	40874,33	23422,35	18190,64	19174,26
11												29320,09	20405,68	19708,35	34947,49	35009,78
12													16307,11	35102,16	59028,7	59575,59
13														20665,23	45657,67	45942,37
14															27422,6	26878,37
15																6883,931
16																

703 Figure 4 **A** tional annotation of pairwise differential expr **B** of treatments

WordCloud representation of GO enrichment analysis of sample pairs. ELICE16INDURES vs Control **(A, B)**, BABA vs Control **(C, D)** and SA vs Control **(E, F)** were compared in time course at the days 0 and 2 and presented in the pairwise Clouds. ELICE16INDURES enhanced the photosynthesis just after addition, which effect was not observed

704

A 705

Pathway	Enzyme	control	SA	BABA	BABA+SA	GOIs PRD AL	AL+SA	AL+BABA	AL+BABA+SA
SA	ICS 2	-45,902	21,2571	66,0767	66,5356	126,055	111,331	67,1239	170,117366
	PAL	34,4533	-21,236	512,28	148,088	20,8041	52,5232	39,5341	24,8926893
JA	AOC	561,764	83,7334	235,493	1183,95	173,431	457,846	1239,62	489,911488
	LOX3	-54,88	78,7676	160,03	168,807	139,252	111,981	306,974	83,2939266
	OPR1	-100	25,1373	-46,812	0	287,361	278,538	612,205	-49,436158
	TIFY11	98,0124	6,77732	12,7932	6,54732	1366	127,976	138,989	665,999
	RHOMBOID	8,79389	9,6754	8,63345	19,4522	789,134	44,765	66,974	67,9983
ABA	ALDO2	-7,7131	-22,945	-8,8206	287,398	39,9708	58,986	96,4704	133,283179
	NCED1	-14,367	-20,991	-18,999	-9,8872	-79,928	-59,28	-68,402	-46,316538
	ZEP1	254,517	317,124	134,027	54,9593	-100	66,5568	149,734	76,9734464
GSH	APX	41,2231	26,7731	245,003	344,013	-18,631	147,616	104,759	-8,2359908
	DHAR	30,0989	79,3916	283,352	132,911	22,2558	124,728	153,357	118,288169
	GPX4	-0,6876	39,1707	32,1396	-1,7503	51,7776	54,3554	67,0673	75,8533613
	GSS	0	0	0	0	0	-100	0	0
	GR	64,1972	-5,3583	1548,83	1504,94	184,824	557,142	699,414	165,46017
AOE	SOD	-100	-67,497	-57,45	21,7538	36,7157	178,226	186,732	-87,933629
	CAT	-5,4622	13,7612	126,935		219,003	217,972	485,026	241,305932

706
707

B

708
709
710

C

711
712
713

Figure 6. Validation analysis of genes of interest (GOI): ABA, JA, SA pathway-related genes, GR, TIFY-domain, and Rhomboid proteins.

PRD values of genes **(A)**. Time course RPM changes as the response of treatments. Since expression intensity of each investigated gene showed high variances - in accordance with their physiological necessities - under control conditions, RPM deviation over days 0. and 2. were determined and expressed in %. Abbreviations: EL, ELICE16INDURES; SA, salicylic acid; BABA, beta-amino butyric acid; ABA, abscisic acid; JA, jasmonic acid; GSH, glutathione metabolism; AOE, antioxidant enzymes.

RT-QPCR validation of SA, JA, ABA, GSH pathway genes treated by priming inducing materials **(B)**.

RT-QPCR validation of TIFY domain proteins and RHOMBOID like 2 protein treated by priming inducing materials **(C)**.
All of investigated priming active materials affected positively the expression of TIFY genes, however, it may be concluded that among them ELICE16INDURES induced most strongly these transcription factors.

The deviations shown in the diagrams are linearly scaled at [min, max] intervals. Min: 0.06, max: 1.96 **(A)**; Min: 0.13 Max: 1.98 **(B)**

714
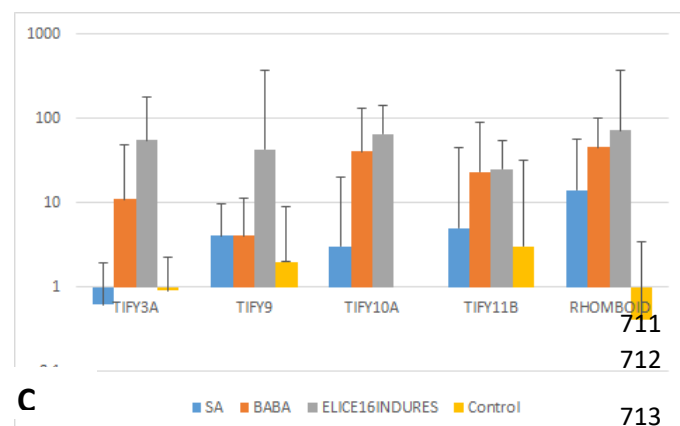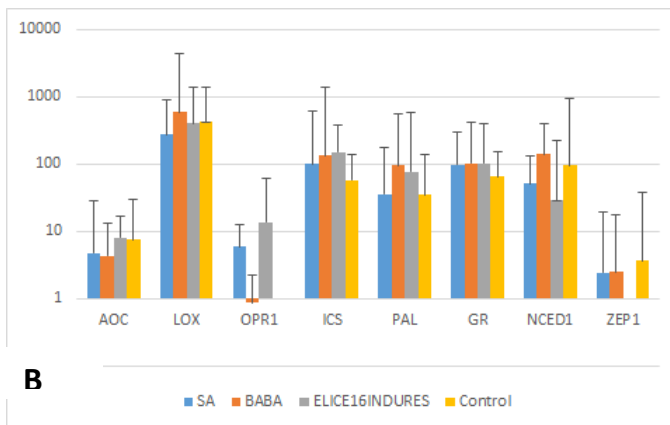
A

$$RPM = \frac{mapped\ reads\ to\ a\ gene\ x\ 10^6}{total\ mapped\ reads}$$

715

716

717

B

$$d(\overrightarrow{vi}; \overrightarrow{vj}) = \sqrt{\sum_{k=1}^{60615}(x_k^i - x_k^j)^2}$$

C

$$\begin{array}{cc} \overrightarrow{vi} & \overrightarrow{vj} \\ x_1^i & x_1^j \\ x_2^i & x_2^j \\ \cdot & \cdot \\ \cdot & \cdot \\ x_n^i & x_n^j \end{array}$$

$$i, j \in \{1; 2; \dots 16\}$$

$$i \neq j$$

718

719

D

$$\sum_{\substack{i,j \in 1..16 \\ i \neq j}} |x_g^i - x_g^j|$$

720

E $$PRD(X_0, X_1) = \begin{cases} 0 & X_0 = 0, X_1 = 0 \\ empty & X_0 = 0, X_1 > 0 \\ 100*(RPM(X_1) - RPM(X_0))/RPM(X_0) & X_0 = 0 \end{cases}$$

721

722

723

724

Figure 7. Formules used for calculations
A. Equation of RPM index used to screening uniquely expressed transcripts and mathematical modeling of interest area. **B.** Equation of distance calculation according to the 2-norm. **C**. 2 elements of the examined n-dimensional vector space, where n = 60,615, ***vi*** and ***vj*** vectors are column vectors of the 1-16 samples in the count table **D**. Equation of change difference of a transcript between the sample pairs. Symbols: **g** is the given transcript of the gene; **xg** is the RPM value that belongs to the transcript; **i,j** are indexes of the sample pairs. **E.** Percentage of relative difference measured by in investigated genes (GOIs). **X0:** RPM value on day zero, **X1:** RPM value on day second, PRD: percentage relative difference

725

Parsed Citations

Abdel-Aziz, H., Hasaneen, M., and Omer, A. (2019). Impact of engineered nanomaterials either alone or loaded with NPK on growth and productivity of French bean plants: Seed priming vs foliar application. South African Journal of Botany 125, 102-108.
Google Scholar: Author Only Title Only Author and Title

Adam, Z. (2015). Plastid intramembrane proteolysis. Biochimica et Biophysica Acta (BBA)-Bioenergetics 1847, 910-914.
Google Scholar: Author Only Title Only Author and Title

Adeniyi, S., Orjiekwe, C., Ehiagbonare, J., and Arimah, B. (2010). Preliminary phytochemical analysis and insecticidal activity of ethanolic extracts of four tropical plants (Vernonia amygdalina, Sida acuta, Ocimum gratissimum and Telfaria occidentalis) against beans weevil (Acanthscelides obtectus). International Journal of Physical Sciences 5, 753-762.
Google Scholar: Author Only Title Only Author and Title

Ahmed, I.M., Cao, F., Zhang, M., Chen, X., Zhang, G., and Wu, F. (2013). Difference in yield and physiological features in response to drought and salinity combined stress during anthesis in Tibetan wild and cultivated barleys. PloS one 8, e77869.
Google Scholar: Author Only Title Only Author and Title

Altschul, S.F., Gish, W., Miller, W., Myers, E.W., and Lipman, D.J. (1990). Basic local alignment search tool. Journal of molecular biology 215, 403-410.
Google Scholar: Author Only Title Only Author and Title

Anders, S., Pyl, P.T., and Huber, W. (2015). HTSeq-a Python framework to work with high-throughput sequencing data. bioinformatics 31, 166-169.
Google Scholar: Author Only Title Only Author and Title

Andrews, S., Krueger, F., Seconds-Pichon, A, Biggins, F., and Wingett, S. (2010). FastQC: a quality control tool for high throughput sequence data. Babraham Bioinformatics. 2010.
Google Scholar: Author Only Title Only Author and Title

Aranega-Bou, P., de la O Leyva, M., Finiti, I., García-Agustín, P., and González-Bosch, C. (2014). Priming of plant resistance by natural compounds. Hexanoic acid as a model. Frontiers in plant science 5, 488.
Google Scholar: Author Only Title Only Author and Title

Arif, Y., Sami, F., Siddiqui, H., Bajguz, A, and Hayat, S. (2020). Salicylic acid in relation to other phytohormones in plant: a study towards physiology and signal transduction under challenging environment. Environmental and Experimental Botany, 104040.
Google Scholar: Author Only Title Only Author and Title

Azami-Sardooei, Z., França, S.C., De Vleesschauwer, D., and Höfte, M. (2010). Riboflavin induces resistance against Botrytis cinerea in bean, but not in tomato, by priming for a hydrogen peroxide-fueled resistance response. Physiological and Molecular Plant Pathology 75, 23-29.
Google Scholar: Author Only Title Only Author and Title

Beckers, G.J., and Conrath, U. (2007). Priming for stress resistance: from the lab to the field. Current opinion in plant biology 10, 425-431.
Google Scholar: Author Only Title Only Author and Title

Bolger, A.M., Lohse, M., and Usadel, B. (2014). Trimmomatic: a flexible trimmer for Illumina sequence data. Bioinformatics 30, 2114-2120.
Google Scholar: Author Only Title Only Author and Title

Brenya, E., Chen, Z.-H., Tissue, D., Papanicolaou, A, and Cazzonelli, C.I. (2020). Prior exposure of Arabidopsis seedlings to mechanical stress heightens jasmonic acid-mediated defense against necrotrophic pathogens. BMC Plant Biology 20, 1-16.
Google Scholar: Author Only Title Only Author and Title

Burketova, L., Trda, L., Ott, P.G., and Valentova, O. (2015). Bio-based resistance inducers for sustainable plant protection against pathogens. Biotechnology advances 33, 994-1004.
Google Scholar: Author Only Title Only Author and Title

Caarls, L., Pieterse, C.M., and Van Wees, S. (2015). How salicylic acid takes transcriptional control over jasmonic acid signaling. Frontiers in plant science 6, 170.
Google Scholar: Author Only Title Only Author and Title

Calvo, P., Nelson, L., and Kloepper, J.W. (2014). Agricultural uses of plant biostimulants. Plant and soil 383, 3-41.
Google Scholar: Author Only Title Only Author and Title

Chen, Z., and Gallie, D.R. (2006). Dehydroascorbate reductase affects leaf growth, development, and function. Plant Physiology 142, 775-787.
Google Scholar: Author Only Title Only Author and Title

Chini, A, Fonseca, S., Fernandez, G., Adie, B., Chico, J., Lorenzo, O., García-Casado, G., López-Vidriero, I., Lozano, F., and Ponce, M. (2007). The JAZ family of repressors is the missing link in jasmonate signalling. Nature 448, 666-671.
Google Scholar: Author Only Title Only Author and Title

Chung, H.S., and Howe, G.A. (2009). A critical role for the TIFY motif in repression of jasmonate signaling by a stabilized splice variant of the JASMONATE ZIM-domain protein JAZ10 in Arabidopsis. The Plant Cell 21, 131-145.
Google Scholar: Author Only Title Only Author and Title

Dangl, J.L., and Jones, J.D. (2001). Plant pathogens and integrated defence responses to infection. nature 411, 826-833.
Google Scholar: Author Only Title Only Author and Title

Divya, B., Suman, B., Venkataswamy, M., and Thyagaraju, K. (2017). A study on phytochemicals, functional groups and mineral composition of Allium sativum (garlic) cloves. International Journal of Current Pharmaceutical Research 9, 42-45.
Google Scholar: Author Only Title Only Author and Title

Du Jardin, P. (2015). Plant biostimulants: definition, concept, main categories and regulation. Scientia Horticulturae 196, 3-14.
Google Scholar: Author Only Title Only Author and Title

Dutta, P. (2018). Seed priming: new vistas and contemporary perspectives. In Advances in seed priming (Springer), pp. 3-22.
Google Scholar: Author Only Title Only Author and Title

Farooq, M., Usman, M., Nadeem, F., ur Rehman, H., Wahid, A., Basra, S.M., and Siddique, K.H. (2019). Seed priming in field crops: potential benefits, adoption and challenges. Crop and Pasture Science 70, 731-771.
Google Scholar: Author Only Title Only Author and Title

Figueiredo, A., Monteiro, F., and Sebastiana, M. (2015). First clues on a jasmonic acid role in grapevine resistance against the biotrophic fungus Plasmopara viticola. European Journal of Plant Pathology 142, 645-652.
Google Scholar: Author Only Title Only Author and Title

Geelen, D., and Xu, L. (2020). The Chemical Biology of Plant Biostimulants. (John Wiley & Sons, Incorporated).
Google Scholar: Author Only Title Only Author and Title

Gill, S.S., Anjum, N.A., Hasanuzzaman, M., Gill, R., Trivedi, D.K., Ahmad, I., Pereira, E., and Tuteja, N. (2013). Glutathione and glutathione reductase: a boon in disguise for plant abiotic stress defense operations. Plant Physiology and Biochemistry 70, 204-212.
Google Scholar: Author Only Title Only Author and Title

Grabherr, M.G., Haas, B.J., Yassour, M., Levin, J.Z., Thompson, D.A., Amit, I., Adiconis, X., Fan, L., Raychowdhury, R., and Zeng, Q. (2011). Trinity: reconstructing a full-length transcriptome without a genome from RNA-Seq data. Nature biotechnology 29, 644.
Google Scholar: Author Only Title Only Author and Title

Guo, Q., Meng, L., Mao, P.-C., Jia, Y.-Q., and Shi, Y.-J. (2013). Role of exogenous salicylic acid in alleviating cadmium-induced toxicity in Kentucky bluegrass. Biochemical Systematics and Ecology 50, 269-276.
Google Scholar: Author Only Title Only Author and Title

Hakata, M., Muramatsu, M., Nakamura, H., Hara, N., Kishimoto, M., Iida-Okada, K., Kajikawa, M., Imai-Toki, N., Toki, S., and Nagamura, Y. (2017). Overexpression of TIFY genes promotes plant growth in rice through jasmonate signaling. Bioscience, biotechnology, and biochemistry 81, 906-913.
Google Scholar: Author Only Title Only Author and Title

Han, L.-m., Hua, W.-p., Cao, X.-y., Yan, J.-a., Chen, C., and Wang, Z.-z. (2020). Genome-wide identification and expression analysis of the superoxide dismutase (SOD) gene family in Salvia miltiorrhiza. Gene 742, 144603.
Google Scholar: Author Only Title Only Author and Title

Harb, A., Awad, D., and Samarah, N. (2015). Gene expression and activity of antioxidant enzymes in barley (Hordeum vulgare L.) under controlled severe drought. Journal of Plant Interactions 10, 109-116.
Google Scholar: Author Only Title Only Author and Title

Heberle, H., Meirelles, G.V., da Silva, F.R., Telles, G.P., and Minghim, R. (2015). InteractiVenn: a web-based tool for the analysis of sets through Venn diagrams. BMC bioinformatics 16, 1-7.
Google Scholar: Author Only Title Only Author and Title

Huang, D.W., Sherman, B.T., and Lempicki, R.A. (2009). Bioinformatics enrichment tools: paths toward the comprehensive functional analysis of large gene lists. Nucleic acids research 37, 1-13.
Google Scholar: Author Only Title Only Author and Title

Kalbi, S., Fallah, A., and Shataee, S. (2014). Estimation of forest attributes in the Hyrcanian forests, comparison of advanced space-borne thermal emission and reflection radiometer and satellite poure l'observation de la terre-high resolution grounding data by multiple linear, and classification and regression tree regression models. Journal of Applied Remote Sensing 8, 083632.
Google Scholar: Author Only Title Only Author and Title

Kanaoka, M.M., Urban, S., Freeman, M., and Okada, K. (2005). An Arabidopsis Rhomboid homolog is an intramembrane protease in plants. FEBS letters 579, 5723-5728.
Google Scholar: Author Only Title Only Author and Title

Karny, A., Zinger, A., Kajal, A., Shainsky-Roitman, J., and Schroeder, A. (2018). Therapeutic nanoparticles penetrate leaves and deliver nutrients to agricultural crops. Scientific Reports 8, 1-10.
Google Scholar: Author Only Title Only Author and Title

Khan, A., Numan, M., Khan, A.L., Lee, I.-J., Imran, M., Asaf, S., and Al-Harrasi, A. (2020). Melatonin: Awakening the defense mechanisms during plant oxidative stress. Plants 9, 407.
Google Scholar: Author Only Title Only Author and Title

Khan, M.I.R., Fatma, M., Per, T.S., Anjum, N.A., and Khan, N.A. (2015). Salicylic acid-induced abiotic stress tolerance and underlying mechanisms in plants. Frontiers in plant science 6, 462.
Google Scholar: Author Only Title Only Author and Title

Klokić, I., Koleška, I., Hasanagić, D., Murtić, S., Bosančić, B., and Todorović, V. (2020). Biostimulants' influence on tomato fruit characteristics at conventional and low-input NPK regime. Acta Agriculturae Scandinavica, Section B-Soil & Plant Science 70, 233-240.
Google Scholar: Author Only Title Only Author and Title

Knopf, R.R., Feder, A., Mayer, K., Lin, A., Rozenberg, M., Schaller, A., and Adam, Z. (2012). Rhomboid proteins in the chloroplast envelope affect the level of allene oxide synthase in Arabidopsis thaliana. The Plant Journal 72, 559-571.
Google Scholar: Author Only Title Only Author and Title

Koressaar, T., and Remm, M. (2007). Enhancements and modifications of primer design program Primer3. Bioinformatics 23, 1289-1291.
Google Scholar: Author Only Title Only Author and Title

Langmead, B., and Salzberg, S.L. (2012). Fast gapped-read alignment with Bowtie 2. Nature methods 9, 357.
Google Scholar: Author Only Title Only Author and Title

Latif, S., Gurusinghe, S., Weston, P.A., Quinn, J.C., Piltz, J.W., and Weston, L.A. (2020). Metabolomic approaches for the identification of flavonoids associated with weed suppression in selected Hardseeded annual pasture legumes. Plant and Soil 447, 199-218.
Google Scholar: Author Only Title Only Author and Title

Liu, S., Li, M., Su, L., Ge, K., Li, L., Li, X., Liu, X., and Li, L. (2016). Negative feedback regulation of ABA biosynthesis in peanut (Arachis hypogaea): a transcription factor complex inhibits AhNCED1 expression during water stress. Scientific reports 6, 1-11.
Google Scholar: Author Only Title Only Author and Title

Lu, Y., and Yao, J. (2018). Chloroplasts at the crossroad of photosynthesis, pathogen infection and plant defense. International journal of molecular sciences 19, 3900.
Google Scholar: Author Only Title Only Author and Title

Maksymiec, W., Wianowska, D., Dawidowicz, A.L., Radkiewicz, S., Mardarowicz, M., and Krupa, Z. (2005). The level of jasmonic acid in Arabidopsis thaliana and Phaseolus coccineus plants under heavy metal stress. Journal of plant physiology 162, 1338-1346.
Google Scholar: Author Only Title Only Author and Title

Mátyás, K.K., Hegedűs, G., Taller, J., Farkas, E., Decsi, K., Kutasy, B., Kálmán, N., Nagy, E., Kolics, B., and Virág, E. (2019). Different expression pattern of flowering pathway genes contribute to male or female organ development during floral transition in the monoecious weed Ambrosia artemisiifolia L.(Asteraceae). PeerJ 7, e7421.
Google Scholar: Author Only Title Only Author and Title

Mayer, L.D., Bally, M.B., Hope, M.J., and Cullis, P.R. (1986). Techniques for encapsulating bioactive agents into liposomes. Chemistry and physics of lipids 40, 333-345.
Google Scholar: Author Only Title Only Author and Title

Moses, T., Papadopoulou, K.K., and Osbourn, A. (2014). Metabolic and functional diversity of saponins, biosynthetic intermediates and semi-synthetic derivatives. Critical reviews in biochemistry and molecular biology 49, 439-462.
Google Scholar: Author Only Title Only Author and Title

Mou, Z., Fan, W., and Dong, X. (2003). Inducers of plant systemic acquired resistance regulate NPR1 function through redox changes. Cell 113, 935-944.
Google Scholar: Author Only Title Only Author and Title

Mujeeb, F., Bajpai, P., and Pathak, N. (2014). Phytochemical evaluation, antimicrobial activity, and determination of bioactive components from leaves of Aegle marmelos. BioMed research international 2014.
Google Scholar: Author Only Title Only Author and Title

Narwal, S. (2006). Allelopathy in ecological sustainable agriculture. In Allelopathy (Springer), pp. 537-564.
Google Scholar: Author Only Title Only Author and Title

Narwal, S.S. (2012). Allelopathy in crop production. (Scientific publishers).
Google Scholar: Author Only Title Only Author and Title

Noutoshi, Y., Okazaki, M., Kida, T., Nishina, Y., Morishita, Y., Ogawa, T., Suzuki, H., Shibata, D., Jikumaru, Y., and Hanada, A. (2012). Novel plant immune-priming compounds identified via high-throughput chemical screening target salicylic acid glucosyltransferases in Arabidopsis. The Plant Cell 24, 3795-3804.
Google Scholar: Author Only Title Only Author and Title

Olusanmi, M., and Amadi, J. (2010). Studies on the antimicrobial properties and phytochemical screening of garlic (Allium sativum) extracts. Ethnobotanical leaflets 2009, 10.
Google Scholar: Author Only Title Only Author and Title

Parađiković, N., Teklić, T., Zeljković, S., Lisjak, M., and Špoljarević, M. (2019). Biostimulants research in some horticultural plant species-A review. Food and Energy Security 8, e00162.
Google Scholar: Author Only Title Only Author and Title

Pastor, V., Luna, E., Ton, J., Cerezo, M., García-Agustín, P., and Flors, V. (2013). Fine tuning of reactive oxygen species homeostasis regulates primed immune responses in Arabidopsis. Molecular plant-microbe interactions 26, 1334-1344.
Google Scholar: Author Only Title Only Author and Title

Pieczul, K., Dobrzycka, A, Wolko, J., Perek, A, Zie|ezińska, M., Bocianowski, J., and Rybus-Zając, M. (2020). The activity of β-glucosidase and guaiacol peroxidase in different genotypes of winter oilseed rape (Brassica napus L.) infected by Alternaria black spot fungi. Acta Physiologiae Plantarum 42, 1-9.
Google Scholar: Author Only Title Only Author and Title

Prabha, D., Negi, S., Kumari, P., Negi, Y.K., and Chauhan, J. (2016). Effect of seed priming with some plant leaf extract on seedling growth characteristics and root rot disease in tomato. International Journal of Agriculture System 4, 46-51.
Google Scholar: Author Only Title Only Author and Title

Reddy, A.R., Chaitanya, K., Jutur, P., and Sumithra, K. (2004). Differential antioxidative responses to water stress among five mulberry (Morus alba L.) cultivars. Environmental and experimental botany 52, 33-42.
Google Scholar: Author Only Title Only Author and Title

Robinson, M.D., McCarthy, D.J., and Smyth, G.K. (2010). edgeR: a Bioconductor package for differential expression analysis of digital gene expression data. Bioinformatics 26, 139-140.
Google Scholar: Author Only Title Only Author and Title

Ruan, J., Zhou, Y., Zhou, M., Yan, J., Khurshid, M., Weng, W., Cheng, J., and Zhang, K. (2019). Jasmonic acid signaling pathway in plants. International journal of molecular sciences 20, 2479.
Google Scholar: Author Only Title Only Author and Title

Saez, G., Bannister, W., and Bannister, J. (1990). Free radicals and thiol compounds. The role of glutathione against free radical toxicity. (Boca Raton FL: CRC Press Inc).
Google Scholar: Author Only Title Only Author and Title

Satish, S., Mohana, D., Ranhavendra, M., and Raveesha, K. (2007). Antifungal activity of some plant extracts against important seed borne pathogens of Aspergillus sp. Journal of Agricultural technology 3, 109-119.
Google Scholar: Author Only Title Only Author and Title

Schwessinger, B., and Ronald, P.C. (2012). Plant innate immunity: perception of conserved microbial signatures. Annual review of plant biology 63, 451-482.
Google Scholar: Author Only Title Only Author and Title

Sharma, H.S., Fleming, C., Selby, C., Rao, J., and Martin, T. (2014). Plant biostimulants: a review on the processing of macroalgae and use of extracts for crop management to reduce abiotic and biotic stresses. Journal of applied phycology 26, 465-490.
Google Scholar: Author Only Title Only Author and Title

Silverman, P., Seskar, M., Kanter, D., Schweizer, P., Metraux, J.-P., and Raskin, I. (1995). Salicylic acid in rice (biosynthesis, conjugation, and possible role). Plant physiology 108, 633-639.
Google Scholar: Author Only Title Only Author and Title

Singh, S., Kumar, V., Kapoor, D., Kumar, S., Singh, S., Dhanjal, D.S., Datta, S., Samuel, J., Dey, P., and Wang, S. (2020). Revealing on hydrogen sulfide and nitric oxide signals co-ordination for plant growth under stress conditions. Physiologia Plantarum 168, 301-317.
Google Scholar: Author Only Title Only Author and Title

Sousa, R.H., Carvalho, F.E., Ribeiro, C.W., Passaia, G., Cunha, J.R., LIMA-MELO, Y., MARGIS-PINHEIRO, M., and Silveira, J.A. (2015). Peroxisomal APX knockdown triggers antioxidant mechanisms favourable for coping with high photorespiratory H_2O_2 induced by CAT deficiency in rice. Plant, cell & environment 38, 499-513.
Google Scholar: Author Only Title Only Author and Title

Špoljarević, M., Štolfa, I., Lisjak, M., Stanisavljević, A, Vinković, T., Agić, D., Parađiković, N., Teklić, T., Engler, M., and Klešić, K. (2010). Strawberry (Fragaria x ananassa Duch) leaf antioxidative response to biostimulators and reduced fertilization with N and K. Poljoprivreda 16, 50-56.
Google Scholar: Author Only Title Only Author and Title

Taheri, P., and Tarighi, S. (2010). Riboflavin induces resistance in rice against Rhizoctonia solani via jasmonate-mediated priming of phenylpropanoid pathway. Journal of plant physiology 167, 201-208.
Google Scholar: Author Only Title Only Author and Title

Thines, B., Katsir, L., Melotto, M., Niu, Y., Mandaokar, A, Liu, G., Nomura, K., He, S.Y., Howe, G.A, and Browse, J. (2007). JAZ repressor proteins are targets of the SCF COI1 complex during jasmonate signalling. Nature 448, 661-665.
Google Scholar: Author Only Title Only Author and Title

Toscano, S., Romano, D., Massa, D., Bulgari, R., Franzoni, G., and Ferrante, A. (2018). Biostimulant applications in low input horticultural cultivation systems= I biostimolanti nei sistemi colturali ortofloricoli a basso impatto ambientale.

Ugena, L., Hýlová, A, Podlešáková, K., Humplík, J.F., Doležal, K., Diego, N.D., and Spíchal, L. (2018). Characterization of biostimulant mode of action using novel multi-trait high-throughput screening of Arabidopsis germination and rosette growth. Frontiers in plant science 9, 1327.

Google Scholar: Author Only Title Only Author and Title

Untergasser, A, Cutcutache, I., Koressaar, T., Ye, J., Faircloth, B.C., Remm, M., and Rozen, S.G. (2012). Primer3-new capabilities and interfaces. Nucleic acids research 40, e115-e115.

Google Scholar: Author Only Title Only Author and Title

Vanholme, B., Grunewald, W., Bateman, A, Kohchi, T., and Gheysen, G. (2007). The tify family previously known as ZIM. Trends in plant science 12, 239-244.

Google Scholar: Author Only Title Only Author and Title

Vargas-Hernandez, M., Macias-Bobadilla, I., Guevara-Gonzalez, R.G., Romero-Gomez, S.d.J., Rico-Garcia, E., Ocampo-Velazquez, R.V., Alvarez-Arquieta, L.d.L., and Torres-Pacheco, I. (2017). Plant hormesis management with biostimulants of biotic origin in agriculture. Frontiers in plant science 8, 1762.

Google Scholar: Author Only Title Only Author and Title

Virág, E., Hegedűs, G., Barta, E., Nagy, E., Mátyás, K., Kolics, B., and Taller, J. (2016). Illumina sequencing of common (short) ragweed (Ambrosia artemisiifolia L.) reproductive organs and leaves. Frontiers in plant science 7, 1506.

Google Scholar: Author Only Title Only Author and Title

Walters, D.R., Newton, A.C., and Lyon, G.D. (2014). Induced resistance for plant defense: a sustainable approach to crop protection. (John Wiley & Sons).

Google Scholar: Author Only Title Only Author and Title

Wang, W., Zhang, G., Yang, S., Zhang, J., Deng, Y., Qi, J., Wu, J., Fu, D., Wang, W., and Hao, Q. (2021). Overexpression of isochorismate synthase enhances drought tolerance in barley. Journal of Plant Physiology, 153404.

Google Scholar: Author Only Title Only Author and Title

Wendehenne, D., Gao, Q.-m, Kachroo, A, and Kachroo, P. (2014). Free radical-mediated systemic immunity in plants. Current opinion in plant biology 20, 127-134.

Google Scholar: Author Only Title Only Author and Title

Wildermuth, M.C., Dewdney, J., Wu, G., and Ausubel, F.M. (2001). Isochorismate synthase is required to synthesize salicylic acid for plant defence. Nature 414, 562-565.

Google Scholar: Author Only Title Only Author and Title

Wu, G., Shortt, B.J., Lawrence, E.B., Leon, J., Fitzsimmons, K.C., Levine, E.B., Raskin, I., and Shah, D.M. (1997). Activation of host defense mechanisms by elevated production of H2O2 in transgenic plants. Plant Physiology 115, 427-435.

Google Scholar: Author Only Title Only Author and Title

Zhang, Y., Fan, W., Kinkema, M., Li, X., and Dong, X. (1999). Interaction of NPR1 with basic leucine zipper protein transcription factors that bind sequences required for salicylic acid induction of the PR-1 gene. Proceedings of the National Academy of Sciences 96, 6523-6528.

Google Scholar: Author Only Title Only Author and Title

Dangl, J.L., and Jones, J.D. (2001). Plant pathogens and integrated defence responses to infection. nature 411, 826-833.

Google Scholar: Author Only Title Only Author and Title

Mou, Z, Fan, W., and Dong, X. (2003). Inducers of plant systemic acquired resistance regulate NPR1 function through redox changes. Cell 113, 935-944.

Google Scholar: Author Only Title Only Author and Title

Wendehenne, D., Gao, Q.-m., Kachroo, A, and Kachroo, P. (2014). Free radical-mediated systemic immunity in plants. Current opinion in plant biology 20, 127-134.

Google Scholar: Author Only Title Only Author and Title

Wu, G., Shortt, B.J., Lawrence, E.B., Leon, J., Fitzsimmons, K.C., Levine, E.B., Raskin, I., and Shah, D.M. (1997). Activation of host defense mechanisms by elevated production of H2O2 in transgenic plants. Plant Physiology 115, 427-435.

Google Scholar: Author Only Title Only Author and Title

Zhang, Y., Fan, W., Kinkema, M., Li, X., and Dong, X. (1999). Interaction of NPR1 with basic leucine zipper protein transcription factors that bind sequences required for salicylic acid induction of the PR-1 gene. Proceedings of the National Academy of Sciences 96, 6523-6528.

Google Scholar: Author Only Title Only Author and Title

Vanholme, B., Grunewald, W., Bateman, A, Kohchi, T., and Gheysen, G. (2007). The tify family previously known as ZIM. Trends in plant science 12, 239-244.

Google Scholar: Author Only Title Only Author and Title

Chini, A, Fonseca, S., Fernandez, G., Adie, B., Chico, J., Lorenzo, O., García-Casado, G., López-Vidriero, I., Lozano, F., and Ponce, M. (2007). The JAZ family of repressors is the missing link in jasmonate signalling. Nature 448, 666-671.

Google Scholar: Author Only Title Only Author and Title

Thines, B., Katsir, L., Melotto, M., Niu, Y., Mandaokar, A, Liu, G., Nomura, K., He, S.Y., Howe, G.A, and Browse, J. (2007). JAZ repressor proteins are targets of the SCF COI1 complex during jasmonate signalling. Nature 448, 661-665.

Google Scholar: Author Only Title Only Author and Title